1957-05

A passive element nonlinear controller for torque-saturating servos

Minnis, M. L.

University of Michigan, 1957.

A PASSIVE ELEMENT NONLINEAR CONTROLLER FOR TORQUE-SATURATING SERVOS

H. D. PARODE
AND M. L. MINNIS

A PASSIVE ELEMENT NONLINEAR CONTROLLER FOR TORQUE-SATURATING SERVOS

by

M. L. Minnis

and

H. D. Parode

MAY 1957

TABLE OF CONTENTS

A PASSIVE NONLINEAR ELEMENT CONTROLLER

FOR TORQUE-SATURATING SERVOS

SUMMARY

This study was made to investigate the use of a particular type of nonlinear control for a torque-saturating second-order servomechanism. The controller utilizes germanium diodes, a Thyrite resistor, standard linear resistors, and capacitors. The Thyrite allows approximation of a torque switching curve with a region of unsaturated operation about the curve. The switching curve gives prediction to obtain optimum time response with little or no overshoot to step and ramp inputs. The controller can use derivative control as well as error-rate control.

The results of simulation on an electronic differential analyzer show marked improvement in response when using prediction as compared to proportional, proportional plus error-rate, or proportional plus derivative control. The use of derivative control instead of error-rate control for prediction necessitates an optimization for either step or ramp inputs.

The system can still handle both types of inputs, but a "best" response, rather than an optimum response as obtained with error-rate control, is realized. This "best" system has very little steady state error to small ramp inputs and

very little deviation from an optimum response to step inputs.

The application of the nonlinear control to an instrument servo system, consisting of a 400 cycle per second, two-phase motor coupled directly to a one-turn potentiometer, substantiated the results obtained by simulation. The characteristics of the film potentiometer permitted the use of a d. c. operational amplifier circuit as a differentiator to form derivative feedback or error-rate feedback. A response time of 0. 05 seconds with no overshoot was obtained to a half-turn step input.

SYMBOLS

C	Capacitance, microfarads unless otherwise indicated
i	subscript meaning input
I	moment of inertia
m	subscript meaning maximum
o	subscript meaning output
R, r	Resistance, megohms unless otherwise indicated
sat	saturation, see Appendix I
t	time, seconds
T	torque, lb.-ft.
TSFS	Torque-Saturating Frictionless Servo, abbreviation
ϵ	error, $\theta_i - \theta_o$, radians
ϵ_ℓ	error to torque-saturate the servo, T_m/μ
$\dot{\epsilon}$	$d\epsilon/dt$
$\ddot{\epsilon}$	$d^2\epsilon/dt^2$
ζ	damping ratio
θ	angular position, radians or volts
μ	gain constant
ω_n	undamped natural frequency, $\omega_n^2 = \mu/I$
ω_c	filter cutoff frequency, rad./sec.
Ω	input angular frequency

A PASSIVE ELEMENT NONLINEAR CONTROLLER FOR TORQUE-SATURATING SERVOS

INTRODUCTION

A servo system designed to operate with infinite acceleration and instantaneous change of direction would be ideal, but is clearly unobtainable. One limitation preventing realization of this ideal is torque saturation (acceleration saturation when the load is purely inertial). Any attempt to operate at maximum acceleration in an approach to the ideal requires a departure from linear control techniques, which naturally increases the complexity of the design.

Considerable work has been done in an attempt to realize some of the improvement in performance apparent with the ideal. One method was to use discontinuous maximum torque operation which gave maximum obtainable system acceleration. McDonald proposed the use of "on-off" or contactor servos, wherein maximum torque of one sign or the other is applied. [A]*

A shorter response time and a greater accuracy than that found in "on-off" operation has been achieved by using a dual-mode controller. [A, B, C] This technique provides a full-torque control region of operation for large amplitude signals plus a region of linear operation when the error signal amplitudes are

---

* Parenthetical superscripts refer to references.

small. A mode selector controlled by ϵ and $\dot{\epsilon}$ is required for this system. The introduction of prediction or switching circuits for torque control to give optimum response to step or ramp inputs has been demonstrated. [A, B, C, D]

W. W. Gay and W. S. McCord furthered previous work by examining a system similar to the dual-mode system just described, but which did not require a mode selector. [E] The control involved mechanization, with diode limitors and operational amplifiers, of an approximate switching curve in the phase plane of error and error-rate with a region of unsaturated operation about this curve. The switching curve was shaped to give optimum time response and essentially no overshoot for step and ramp inputs. The basic theory, as applied to a torque-saturating second order servomechanism, was originally developed by L. L. Rauch and R. M. Howe[F] and it is summarized in Appendix I.

This study is an extension of the work of Gay and McCord to reduce the complexity of the controller by replacing certain active components with passive elements. This study also considers a method for improving servo response by utilizing Thyrite[G, H] to provide a more exact approximation to the switching curve. This use for Thyrite is detailed in Appendix II.

Further, the use of derivative control, as well as error-rate control, is investigated since the latter leads to difficulties in instances where noise appears in the input signal. The high frequency components of the noise result in jerky outputs when high loop gains are used because the differentiated noise signal is added to the error-rate.

Since the use of derivative feedback for damping of a servomechanism results in a steady state error for a constant velocity input, [I] an accompanying

investigation is made to consider the removal or reduction of this error by passing the derivative signal through a high pass filter. The study considers the best filter location and cutoff frequency for both step and ramp inputs.

The investigation was performed by M. L. Minnis and H. D. Parode as a joint project to satisfy, in part, the requirements for a Master of Science Degree in Aeronautical Engineering at the University of Michigan.

SIMULATION

The simulation study was undertaken to provide analog computer solutions of the theoretical equations of a torque-saturating servomechanism. Solutions were first obtained through the full use of d.c. operational amplifiers and a servo multiplier. Following this, solutions were obtained by replacing the servo multiplier with a nonlinear resistor, Thyrite, to provide an approximate prediction curve. The use of Thyrite for this application is developed in Appendix II.

PROCEDURE

The simulations considered were those of a:

(1) Servo using proportional and error-rate control without prediction;

(2) Servo using proportional and derivative control without prediction;

(3) Servo using proportional and error-rate control with prediction;

(4) Servo using proportional and derivative control with prediction;

(5) Servo using proportional control and derivative control through a high pass filter without prediction;

(6) Servo using proportional control and derivative control through a high pass filter with prediction;

(7) Servo using proportional control and derivative control through a high pass filter with Thyrite for prediction.

The equation for a torque-saturating frictionless servo with proportional and error-rate control is:

$$I\ddot{\theta}_o = T_m \text{ sat } \left[\frac{\mu}{T_m}\left(\epsilon + C_e\dot{\epsilon}\right)\right]^{*}, \text{ where } C_e = \frac{2\zeta}{\omega_n}.$$

The equation was time scaled by the undamped natural frequency, ω_n, and magnitude scaled by the error required for torque-saturation, ϵ_ℓ. These quantities are defined as:

$$\omega_n^2 = \frac{\mu}{I}, \text{ and } \epsilon_\ell = \frac{T_m}{\mu}$$

The scaled equation for the computer was:

$$\frac{\ddot{\theta}_o}{\omega_n^2} = \epsilon_\ell \text{ sat } \left[\frac{1}{\epsilon_\ell}\left(\epsilon + \frac{2\zeta\dot{\epsilon}}{\omega_n}\right)\right].$$

100 volts in the computer represented unity in the problem. For this computer representation, arbitrary values were chosen for the equation parameters as follows: $\omega_n = 1.0$, $\zeta = 0.5$, $\epsilon_\ell = 0.025$. The solutions were plotted in dimensionless form as ϵ/ϵ_ℓ versus $\omega_n t$ in the time plots and $\dot{\epsilon}/\omega_n$ versus ϵ/ϵ_ℓ in the phase plane plots.

Fig. 1 is the computer circuit for the solution of the above equation. The high pass filter in Fig. 1 was not connected when error-rate was utilized for control.

The effect of torque-saturating was simulated by limiting with operational amplifiers. (J)

The introduction of prediction modified the servo equation of motion to a form developed in Appendix I. The computer equation was:

---

* This symbol for saturation is explained in Appendix I.

$$I\ddot{\theta}_o = T_m \text{ sat}\left\{ \frac{\mu}{T_m}\left[\epsilon + \frac{T_m}{\mu} \text{ sat}\left(\frac{\mu}{T_m} C_e \dot{\epsilon}\right) + \frac{I}{2T_m}|\dot{\epsilon}|\dot{\epsilon}\right]\right\}$$

The computer scaling procedure and selected values for the equation parameters were the same as before, which resulted in:

$$\frac{\ddot{\theta}_o}{\omega_n^2} = \epsilon_\ell \text{ sat}\left\{\frac{1}{\epsilon_\ell}\left[\epsilon + \epsilon_\ell \text{ sat}\left(\frac{2\zeta}{\epsilon_\ell}\frac{\dot{\epsilon}}{\omega_n}\right) + \frac{1}{2\epsilon_\ell}\left|\frac{\dot{\epsilon}}{\omega_n}\right|\frac{\dot{\epsilon}}{\omega_n}\right]\right\}.$$

Fig. 2 is the computer circuit for this equation with a servo multiplier to form the prediction product, $\left|\frac{\dot{\epsilon}}{\omega_n}\right|\frac{\dot{\epsilon}}{\omega_n}$. This equation was also solved using Thyrite to form the prediction product. No attempt was made to optimize the response for Coulomb or viscous friction effects.

Solutions for ramp inputs using derivative control result in a steady state error. In order to remove this error, the derivative signal is passed through a high pass filter. The cutoff frequency of the filter is made lower than the resonant frequency of the servo so that the necessary damping is provided. The transfer function of the filter, Y_f, is given by:

$$Y_f = \frac{\tau_p}{\tau_p + 1}, \text{ where } \tau = RC = \frac{1}{\omega_c}.$$

Figs. 1 and 2 show simulation of a RC circuit with the desired characteristics to remove any steady state error. The derivative signal is first passed, when varying, to provide the necessary damping for the system. Then it is reduced to zero in a time determined by the time constant of the filter, removing any steady state error. However, response time to a step input is increased when utilizing a filter, since the system damping is reduced. In order to eliminate the steady state error resulting from constant velocity inputs, this increase

in time response to a step input must be accepted when using derivative feedback. Solutions to the simulation problem were obtained for various filter cut-off frequencies and filter locations.

RESULTS AND DISCUSSION

Solutions in the form of phase plane plots and time plots for the various types of control outlined previously were obtained for simulation study. In general, responses to step, ramp and sinusoidal inputs using proportional plus error-rate, then proportional plus derivative, and proportional plus filtered derivative control were recorded. Following this, prediction was introduced, and the above runs repeated. Finally, Thyrite was substituted for the servo multiplier, and responses using proportional control and derivative control through a high pass filter were recorded, for the various inputs.

The improvement in performance due to prediction for step inputs is shown in Figs. 3 through 8. Derivative control gives exactly the same improvement in performance as does error-rate control. This result is important since derivative control might be desirable when input noise precludes differentiation of the error to provide error-rate. The response time varied as the square root of the input magnitudes, since, for a second order servo with inertia only, the servo equation of motion is:

$$I \ddot{\theta}_o = - T_m$$

from which integration yields

$$\dot{\epsilon} = \frac{T_m}{I} t + \dot{\epsilon}(0).$$

Since $\epsilon(0) = 0$, integration once more produces

$$\epsilon = \frac{-T_m}{2I} t^2 + \epsilon(0)$$

where $\epsilon(0)$ is equal to ϵ for $\dot{\epsilon}$ equal to zero. Setting $\epsilon = 0$ gives,

$$t = \sqrt{\frac{2I}{T_m} \epsilon(0)}$$

For a ramp input, the use of derivative control with or without prediction resulted in a steady state error, as shown in Fig. 9. This response can be compared with the optimum response to a ramp input as shown in Fig. 10. The best response with derivative feedback is realized by using a high pass filter on the derivative signal. Fig. 11 shows that the improvement obtained by filtering approaches the optimum response. All feedback terms are filtered before the nonlinear functions of saturation and squaring are performed. Thus, approximately the same improvement in response obtained by using error-rate can be achieved for either step or ramp inputs with derivative control.

Solutions of the servo response using Thyrite for the prediction curve are shown in Figs. 12 through 21. A comparison of the solutions in Figs. 12 and 13 with those of Figs. 3(b) through 6 (b) show no perceptible difference.

It is desirable to obtain the best improvement possible in response for both step and ramp inputs with the same controller. For this condition, it is necessary to leave the filter in the controller in all cases using derivative control.

Figs. 14 through 21 show solutions to both step and ramp inputs while filtering both terms of the feedback damping. It can be seen that improvement in response to a ramp input for a particular filter cutoff frequency results in

considerable degradation in the response to the step input. With this location of the filter, before the nonlinear function generators, it is necessary to choose a filter cutoff frequency that gives a compromise between responses for the two types of inputs considered. The long delay in reducing the error to zero, with even a very low cutoff frequency, deteriorates the value of prediction for step inputs.

If a small steady state error is acceptable for a ramp input, the response to a step input is caused to deviate only slightly from the optimum by locating the filter after the nonlinearity of the saturated derivative signal, and filtering the limited derivative feedback term only. This effect is illustrated in Fig. 22. The size of this error depends upon the magnitude of the input rate as follows:

The servo equation of motion

$$\frac{\ddot{\theta}_o}{\omega_n^2} = \epsilon_\ell \text{sat}\left\{\frac{1}{\epsilon_\ell}\left[\epsilon + \epsilon_\ell \text{sat}\left(\frac{2J}{\epsilon_\ell}\frac{\dot{\epsilon}}{\omega_n}\right) + \frac{1}{2\epsilon_\ell}\left|\frac{\dot{\epsilon}}{\omega_n}\right|\frac{\dot{\epsilon}}{\omega_n}\right]\right\}$$

requires that

$$\epsilon = -\epsilon_\ell \text{sat}\left(\frac{2J}{\epsilon_\ell}\frac{\dot{\epsilon}}{\omega_n}\right) - \frac{1}{2\epsilon_\ell}\left|\frac{\dot{\epsilon}}{\omega_n}\right|\frac{\dot{\epsilon}}{\omega_n}$$

in the steady state for a ramp input. When error-rate is used, the right hand side of the equation becomes zero. For derivative control, the equation becomes

$$\epsilon = \epsilon_\ell \text{sat}\left(\frac{2J}{\epsilon_\ell}\frac{\dot{\theta}_i}{\omega_n}\right) + \frac{1}{2\epsilon_\ell}\left|\frac{\dot{\theta}_i}{\omega_n}\right|\frac{\dot{\theta}_i}{\omega_n}$$

for steady state, since for this condition, $\dot{\theta}_i = \dot{\theta}_o$. Derivative filtering action reduces the first term of the right hand side of the equation to zero, giving

$$\epsilon = \frac{1}{2\epsilon_\ell}\left|\frac{\dot{\theta}_i}{\omega_n}\right|\frac{\dot{\theta}_i}{\omega_n} .$$

From this equation it can be seen that the squaring of inputs with $\frac{\dot{\theta}_i}{\omega_n} \ll 1$, results in extremely small errors for ramp inputs. A filter cutoff frequency, $\omega_c = \omega_n/3$ was determined experimentally to give the best results. This filter has little deteriorating effect on step input response, but is only applicable to systems with small ramp inputs.

Figs. 23 through 26 show the responses of the servo, with and without prediction, and with and without a high pass filter, to sinusoidal inputs. The presence of the filter and an increase in input frequency deteriorates the response markedly.

Figs. 27 through 33 show the convergent characteristics of the system with derivative control, filtered and not filtered. Use of the filter lowers the maximum allowable input amplitude for neutral stability over that level for derivative control without filter. The maximum input frequency in this case, for the system to follow, is $\Omega = \omega_n/3$.

APPLICATION TO AN INSTRUMENT SERVO

A physical system was devised to demonstrate the use of a passive controller with derivative, or error-rate control for prediction. As in the simulation, Thyrite was used for approximating the prediction curve. In addition, germanium diodes were utilized to limit the derivative feedback necessary for the unsaturated region of operation.

SYSTEM DESCRIPTION

Motor. The servo motor was a two-phase, 400 cycle per second, 115 volt Transicoil motor, Type 18M. Rate stall torque - 3.0 oz.-in., moment of inertia - 0.0197 oz.-in.^{2}, stall watts per phase - 18 watts, Coulomb friction - 0.10 oz.-in., coefficient of viscous friction - 0.00285 oz.-in.-sec.

Potentiometer. Output position voltage for feedback was obtained from a three-section, continuous film potentiometer, Model Number 205, manufactured by Computer Instruments Corp. Resistance - 50,000 ohms, total moment of inertia - 0.164 oz.-in.^{2}, total Coulomb friction - 0.895 oz.-in., total viscous friction - negligible.

Diode Limiting Circuit. Germanium diodes were utilized to limit the derivative feedback necessary for the unsaturated region of operation. Clevite CTP 309 Diodes were used. Maximum ratings: 300ma forward current at one volt; 20 volts maximum inverse voltage. This type of diode has a semiconductor crystal and a small-area metal contact. The behavior of this point-contact diode can be interpreted as though it were a p-n junction diode with special geometry.(K) The method of manufacture of the diode creates a p-n junction of extremely small area associated with the metal point. The details

of the diode layout and its equivalent circuit are:

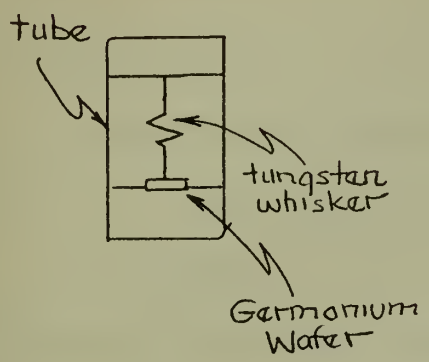

Diode Construction

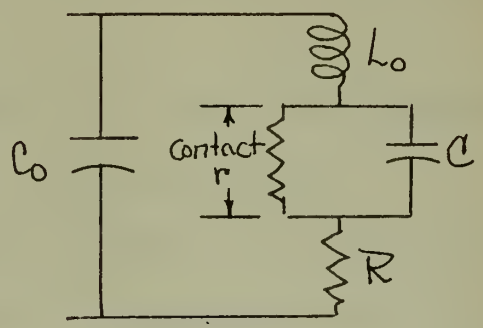

Diode Equivalent Circuit

The effects of the inductance L_o of the tungsten wire and the capacitance C_o of the crystal holder are negligible for this application. When the applied voltage is in the forward direction, the combination of point contact and p-n junction represents a low resistance r, shunted by the barrier capacitance, C. In addition, there is a spreading resistance, R, which takes into account the resistance of the base region to the majority carriers.

When a reverse voltage is applied, only a very small current flows, and the resistance r, is quite large. A contact potential of about 0.2 volts was observed for these diodes. The forward resistance was about 6 ohms, while the back resistance was approximately 200K ohms.

The reverse current is not independent of reverse voltage because of an intense electric field near the contact point and because the carriers tend to travel by drift rather than by diffusion. This effect must be minimized to provide good limiting. Two of these diodes were placed back-to-back in series with a 100K ohm load. The contact potential of the germanium diodes permitted limiting without the use of batteries.

Thyrite for Prediction. General Electric Cat. No. 8396839 G1 Thyrite nonlinear resistors were employed for the squaring damper. This application of Thyrite is detailed in Appendix II.

Compensation and Control Circuits. The remainder of the compensation and control circuits utilized standard resistors and capacitors.

Power Amplifier. An a. c. electronic amplifier in conjunction with a 400 cycle per second chopper to convert the d. c. control signal to 400 cps a. c. signal was used to drive the control phase of the motor. A phase shifter was not required since the chopper altered the phase by about 110 degrees.

Direct coupling of the motor to the potentiometer eliminated the problems of backlash and binding exhibited by gear trains. Although the motor-to-load inertia balance was not ideal, the acceleration loss due to direct coupling was small. The motor-to-load inertia could have been matched by using a three to one gear ratio.

The output voltage was differentiated to form the necessary feedback. This output voltage was converted from the servo output angle by a film potentiometer. Use of a standard wire-wound type of potentiometer would have resulted in jump discontinuities in output voltage as the wiper arm crossed from wire to wire. Differentiation of this signal would produce pulses, causing a very jerky output for the large loop gains required by this controller. The film potentiometer does not exhibit this characteristic and has much less noise and better resolution.

The use of the differentiator permitted the system to be operated using either error-rate or derivative control. A simple RC differentiator could

not be used because of the extreme loss in gain associated with it. The use of a tachometer to obtain the derivative signal would eliminate the necessity for amplification as required by the differentiator.

PROCEDURE

The servo was operated to obtain responses with proportional, proportional plus error-rate control, and proportional plus error-rate control with prediction. The error-rate control was replaced with derivative control, and a comparison of the responses made for step inputs. Further responses were obtained for both step and ramp inputs to investigate the introduction of a high pass filter in the same two locations investigated in the simulation. The filtering is necessary to remove or decrease the steady state error to ramp inputs when using derivative control.

The servo circuit diagram is shown in Fig. 34. The circuit was modified for the various types of control. The servo loop gain was adjusted to the highest possible value consistent with stable operation. Instability probably resulted from a power pickup and the exceeding of the bandwidth limitations of the servo.

The time constants of the approximate differentiating circuit were determined experimentally to limit high frequency noise while retaining the necessary bandwidth. The time constant of 0.0005 seconds corresponds to 319 cycles per second. To further decrease the amount of noise passed, an additional capacitor was inserted in the feedback to give a minus six decibels per octave rolloff of gain for frequencies above 319 cps.

The input voltage, θ_i, and the output voltage, θ_o, were used as references for determining the particular resistors necessary to provide the

correct gain for each signal to the chopper. The chopper input was considered to be ground since its impedance was only 42 ohms. The loss in gain of the differentiator and the insertion loss of the Thyrite were experimentally compensated to obtain satisfactory servo response. A resistor of 0.5 megohms as compared to the reference of one megohm resistance for θ_i, and θ_o, gave the desired gain.

The germanium diodes were matched by measuring the characteristics of several until two were obtained with equal break voltages of about -0.2 and with low reverse current dependence on reverse voltage. The resistance network after the diodes in Fig. 34 acts to obtain the desired gain with respect to the reference voltages, θ_i, and θ_o.

The filter resistance was made small compared to that of the diode and Thyrite networks. This was necessary to prevent the nonlinearities of the saturating and squaring function generators from influencing the filter characteristics, i.e. the cutoff frequency. The presence of the filter in this location also acts to remove any zero drift of the d.c. operational amplifier used in the differentiator.

The inherent system input error was measured by disturbing the servo slightly and noting the error when the output had come to rest. The error was measured as ± 0.005 volts on a voltmeter having a full scale deflection of 0.1 volts.

The velocity error was measured by using a ramp input produced by a 0.5 cycle per second triangular waveform. The transient effects damped out sufficiently to permit measurement of the error before the signal switched.

Photographs of the cathode ray oscilloscope presentation of error versus time for several inputs and types of control were taken. The 100 volt peak-to-peak square wave input had a frequency of 2.5 cps, while the 10 volt peak-to-peak square wave input had a frequency of 5 cps. The ramp input of 440 volts per second was obtained by using a 2 cps triangular wave.

RESULTS AND DISCUSSION

The performance of the servo corresponded to the results of the simulation for both step and ramp inputs. The addition of the high pass filter to remove the steady state error of the ramp input response degraded the response to a step input as demonstrated by the simulation.

The system constant input error was $\pm$ 0.005 volts. The terminal voltages on the potentiometer were $\pm$100 volts with the center tap grounded. With this reference voltage of 200 volts, the constant input error gives a resolution of at least one part in 40,000. Any type of control requiring the differentiator resulted in a noise tracking error to ramp inputs of about 0.5 volts at 200 cps. This noise is plainly evident in Fig. 37(a), and 37(b), where one inch equals 14 volts of error. This noise prevented any measurement of the error of the system with derivative control unless inputs were large compared to the noise amplitude. The noise is probably the result of a power supply pickup which could be eliminated by further study or by the use of a good tachometer.

The poor 400 cps output waveform from the electronic amplifier, though filtered, and the 110 degree phase shift in the chopper, probably produced a somewhat less than rated motor torque. This had negligible effect on the value of the results.

The photographs of the oscilloscope presentations of error or output versus time are shown in Figs. 35 through 37. Prediction eliminated overshoot and greatly reduced the response time. For step inputs, without a filter in the feedback, there was no difference between responses when using error-rate or derivative control. The response times for the 100 volt step input were 0.16, 0.12, and 0.05 seconds for proportional, proportional plus error rate, and proportional plus error-rate with prediction respectively, which compares to 0.17, 0.13, and 0.06 seconds for Gay and McCord's controller on the same servo.(E) A greater improvement with this controller for a 10 volt step input was noted because of the use of the Thyrite, which exhibited a much better approximation to the switching curve at low voltage inputs than the diode circuit of Gay and McCord. The response times for the three types of control were 0.08, 0.045, and 0.03 seconds. This compares with 0.07, 0.035, and 0.035 seconds as obtained from Ref. (E).

Figs. 35(c), and 36(c), show the effect on the optimum prediction response to a step input when the output of the differentiator is filtered. As ω_c was decreased, the oscillations were reduced, but a very long time delay was introduced in returning the error to zero. Figs. 37(a), and 37(b), show the response with the same control configuration, but to a ramp input. It is apparent that as ω_c was decreased, the response time was increased.

Fig. 37(c) shows the response of the system with prediction and a filtering of just the unsaturated region damping term, $\dot{\theta}_o$, to a step input. With $\omega_c = \omega_n/3$, there is little degradation of the step response. This method of control will give a steady state error to a ramp input, but it will

be small if the input rate is small. This is shown for steady state conditions, when the derivative term is filtered out, by the following equation from page 10:

$$\epsilon - \frac{1}{2\epsilon_\ell}\left|\frac{\dot{\theta}_o}{\omega_n}\right|\frac{\dot{\theta}_o}{\omega_n} = 0,$$

where:

$$\dot{\theta}_o = \dot{\theta}_i \qquad \omega_n = 600 \qquad 2\epsilon_\ell = 0.4$$

This yields:

$$\epsilon = 0.695 \times 10^{-5}\left|\dot{\theta}_i\right|\dot{\theta}_i .$$

This steady state error, as calculated from the above equation, is recorded in Table I, for various input rates, with and without the filter in this location.

TABLE I

Steady State Error

$\dot{\theta}_i$ (volts/sec.)	Filtered Term (volts) $(2\zeta/\omega_n\dot{\theta}_o)$	Error Filter In (volts)	Error Filter Out (volts)
5	0.01	0.00^+	0.01
10	0.02	0.00^+	0.02
20	0.03	0.00^+	0.03
40	0.07	0.01	0.08
60	0.10	0.02	0.12
100	0.11	0.07	0.24
150	0.25	0.16	0.41
200	0.42	0.28	0.70
300	0.50	0.70	1.20
400	0.67	1.10	1.77
500	0.83	1.70	2.53

It is apparent from Table I, that for small ramp inputs, the filter in this location appreciably decreases the steady state error. The filtering becomes

ineffective above about 100 volts per second. This error could not be measured because of the before mentioned noise.

Measurements of the velocity error when using proportional control are recorded in Table II.

TABLE II

Velocity Error

$\dot{\theta}_i$ (volts/sec.)	Error (volts)
0.5	0.010
1.0	0.015
3.0	0.025
5.0	0.030
10.0	0.040
20.0	0.060
60.0	0.080
100.0	0.090

The velocity of the motor never exceeded 20% of the maximum allowable. The viscous friction effects of the servo were negligible with this low velocity. The very narrow linear region and a high loop gain made the response of the proportional control servo to a large step input similar to that of a bang-bang servo with Coulomb damping only. The oscillations with proportional control to a step input and the response time with prediction are close to these same parameters calculated for a theoretical bang-bang servo with Coulomb damping.

CONCLUSIONS

SIMULATION

1. Use of prediction reduces response time and overshoot for ramp and step inputs when using error-rate control.

2. Derivative control gives the same performance as error-rate control for step inputs, but results in a steady state error for ramp inputs.

3. Use of a high pass filter before the nonlinear function generators removes the steady state error to ramp inputs.

4. The high pass filter, as located in 3 above, deteriorates the step input optimized response, producing oscillations and a long time response.

5. Use of prediction with derivative control and filtering, as in 3 above, improves the transient response for step sinusoidal inputs, even though the prediction is only optimized for ramp inputs.

6. A high pass filter on the limited derivative feedback term only, results in very small steady state errors and does not greatly effect the optimized step response. This steady state error increases with increasing ramp inputs.

7. The use of Thyrite to approximate the switching curve did not degrade the improvement in performance.

APPLICATION

1. Noise level in the output signal from the film potentiometer was low, permitting differentiation with an operational amplifier to obtain derivative or error-rate control.

2. When using error-rate control, use of the simplified mechanization

gave results better than those achieved in Ref. (E).

3. Filtered derivative control can be used in place of error-rate control without loss in performance for either ramp or step inputs, but not both.

4. When using derivative control, filtering of the derivative terms before the nonlinearities is required to remove all of the steady state error to ramp inputs.

5. Derivative control systems can not be optimized for both ramp and step inputs using this type of controller.

6. A best compromise system, using derivative control, for both ramp and step inputs can be achieved by filtering only the limited derivative feedback term, resulting in very little steady state error with ramp inputs, and little degradation to the optimized step response.

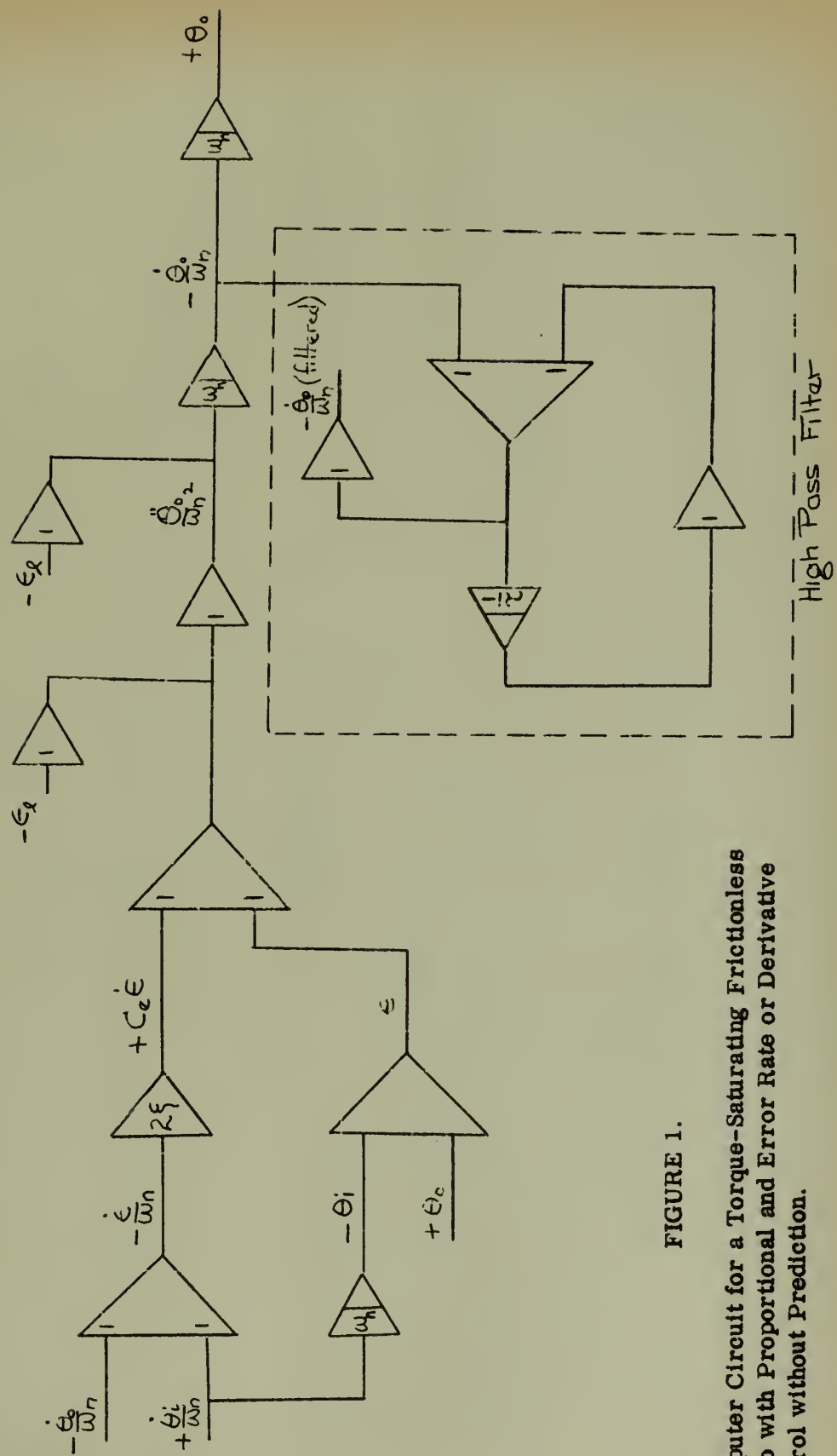

FIGURE 1.

Computer Circuit for a Torque-Saturating Frictionless Servo with Proportional and Error Rate or Derivative Control without Prediction.

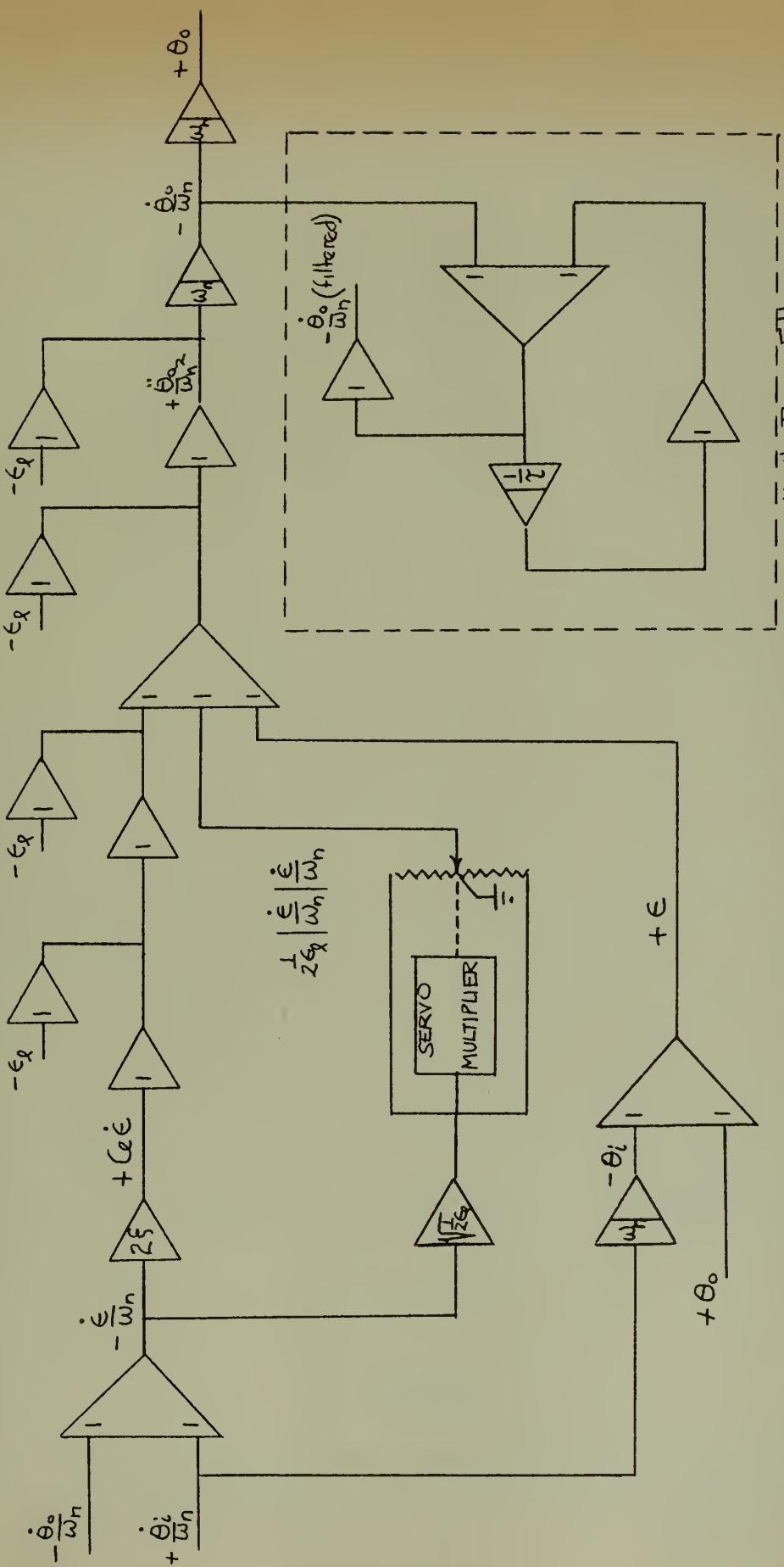

FIGURE 2. Computer Circuit for a Torque-Saturating Frictionless Servo with Proportional and Error Rate or Derivative Control with Prediction.

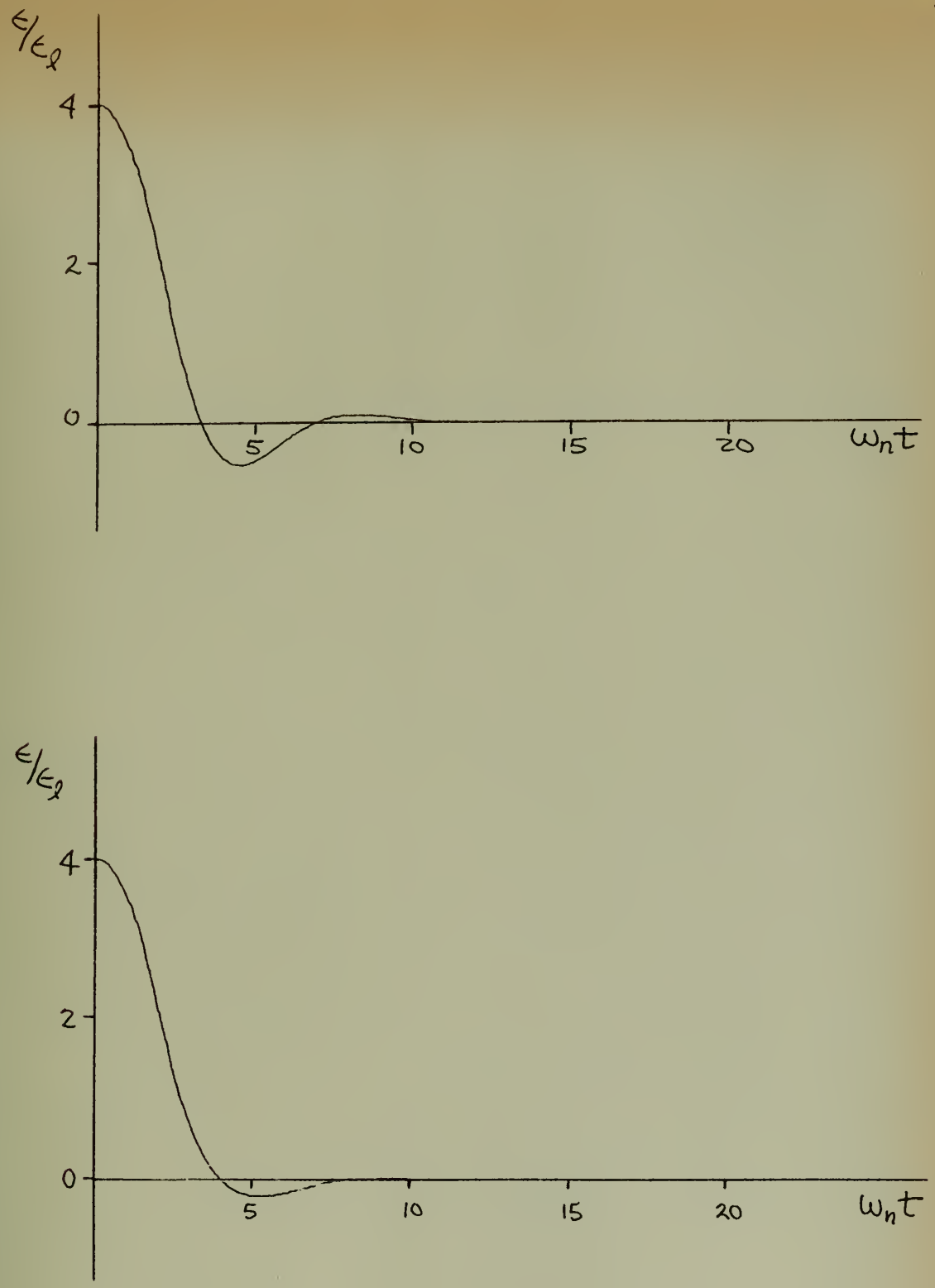

FIGURE 3.

Step Response of a Torque-Saturating Frictionless Servo with Derivative Control, $\zeta = 0.5$, $\omega_n = 1.0$
(a) Without Prediction (b) With Prediction.

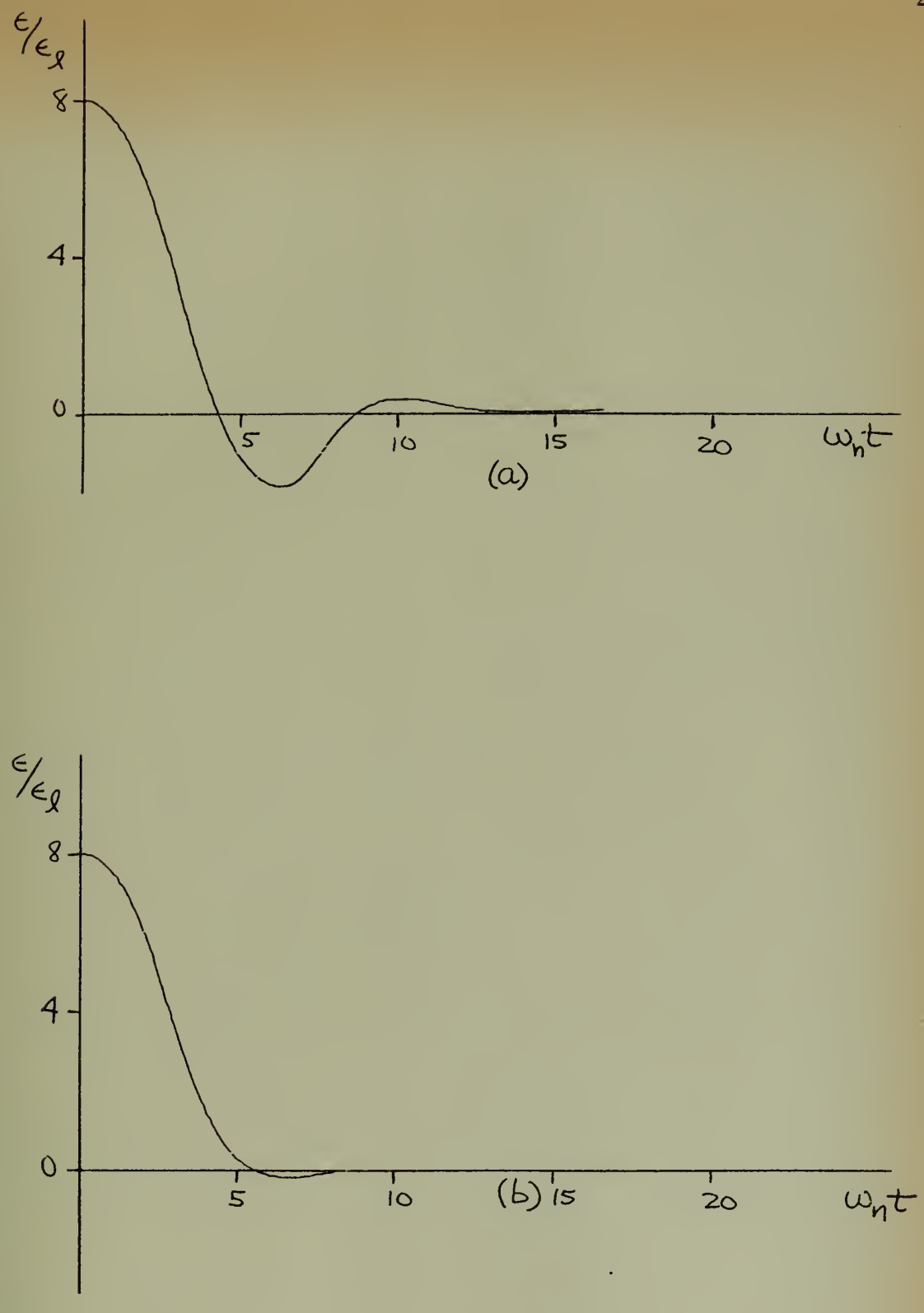

FIGURE 4.

Step Response of a Torque-Saturating Frictionless Servo with Derivative Control, $\zeta = 0.5$, $\omega_n = 1.0$
(a) Without Prediction (b) With Prediction.

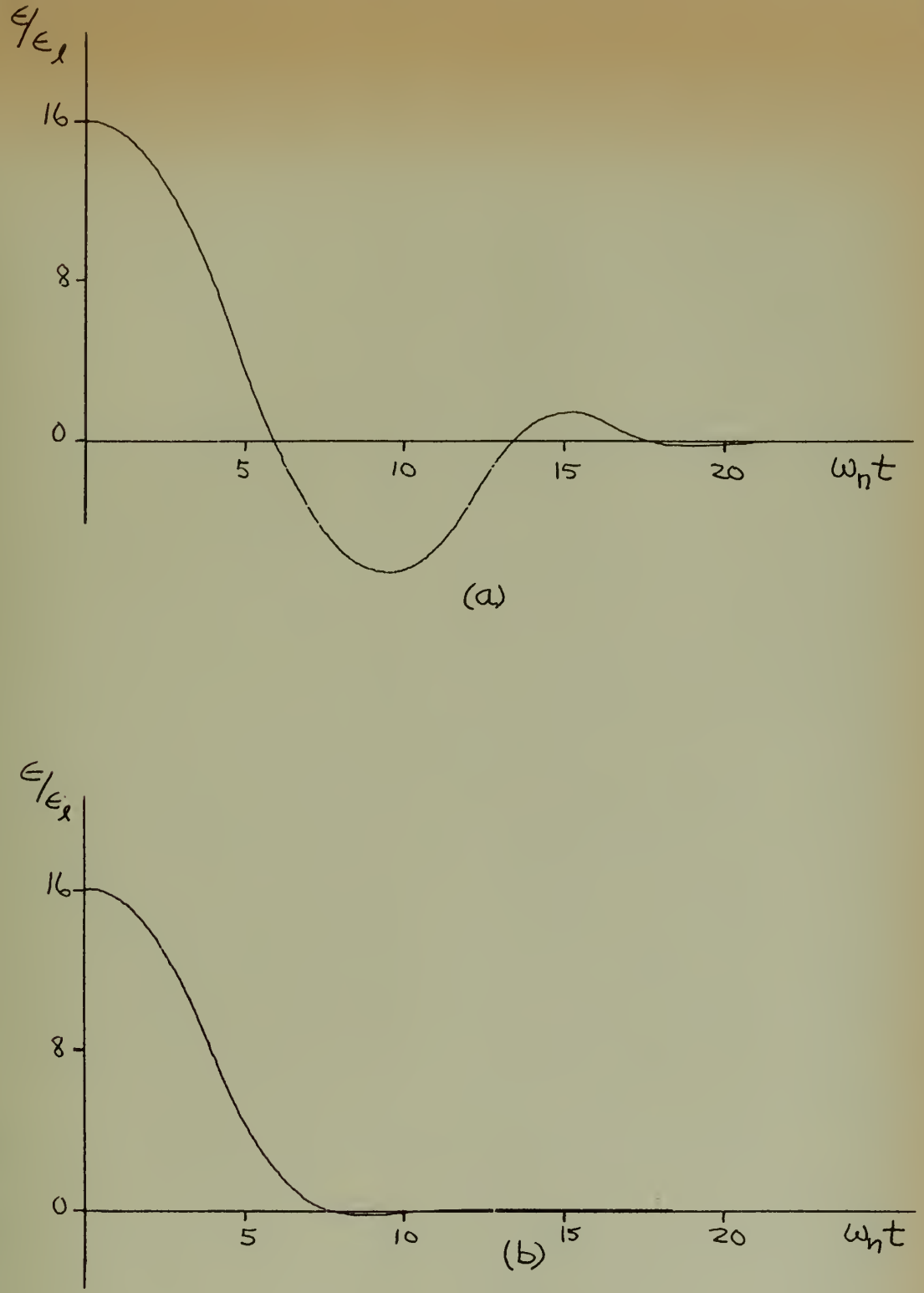

FIGURE 5.

Step Response of a Torque-Saturating Frictionless Servo with Derivative Control, $\zeta = 0.5$, $\omega_n = 1.0$
(a) Without Prediction (b) With Prediction.

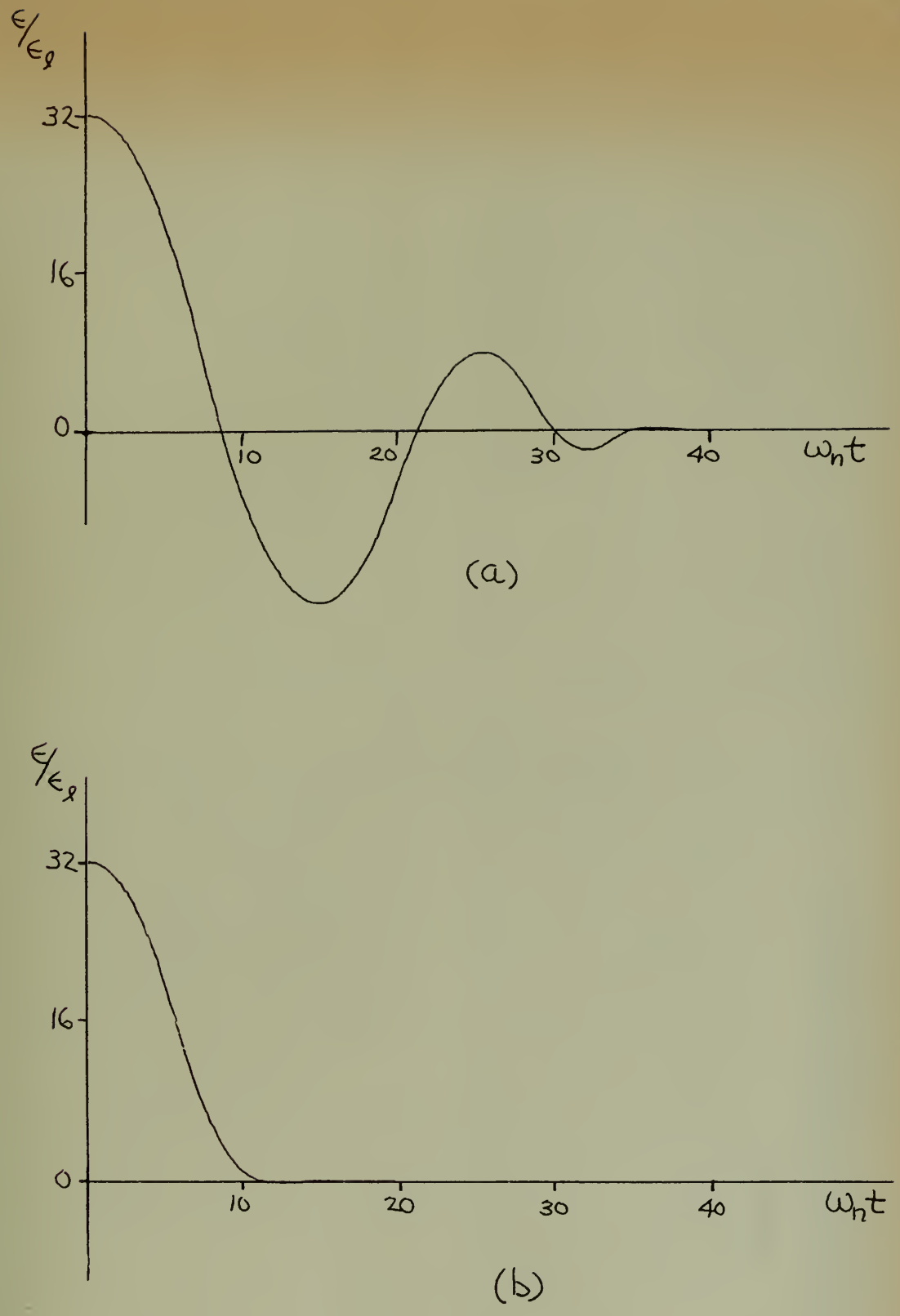

FIGURE 6.

Step Response of a Torque-Saturating Frictionless Serve with Derivative Control, $\zeta = 0.5$, $\omega_n = 1.0$
(a) Without Prediction (b) With Prediction.

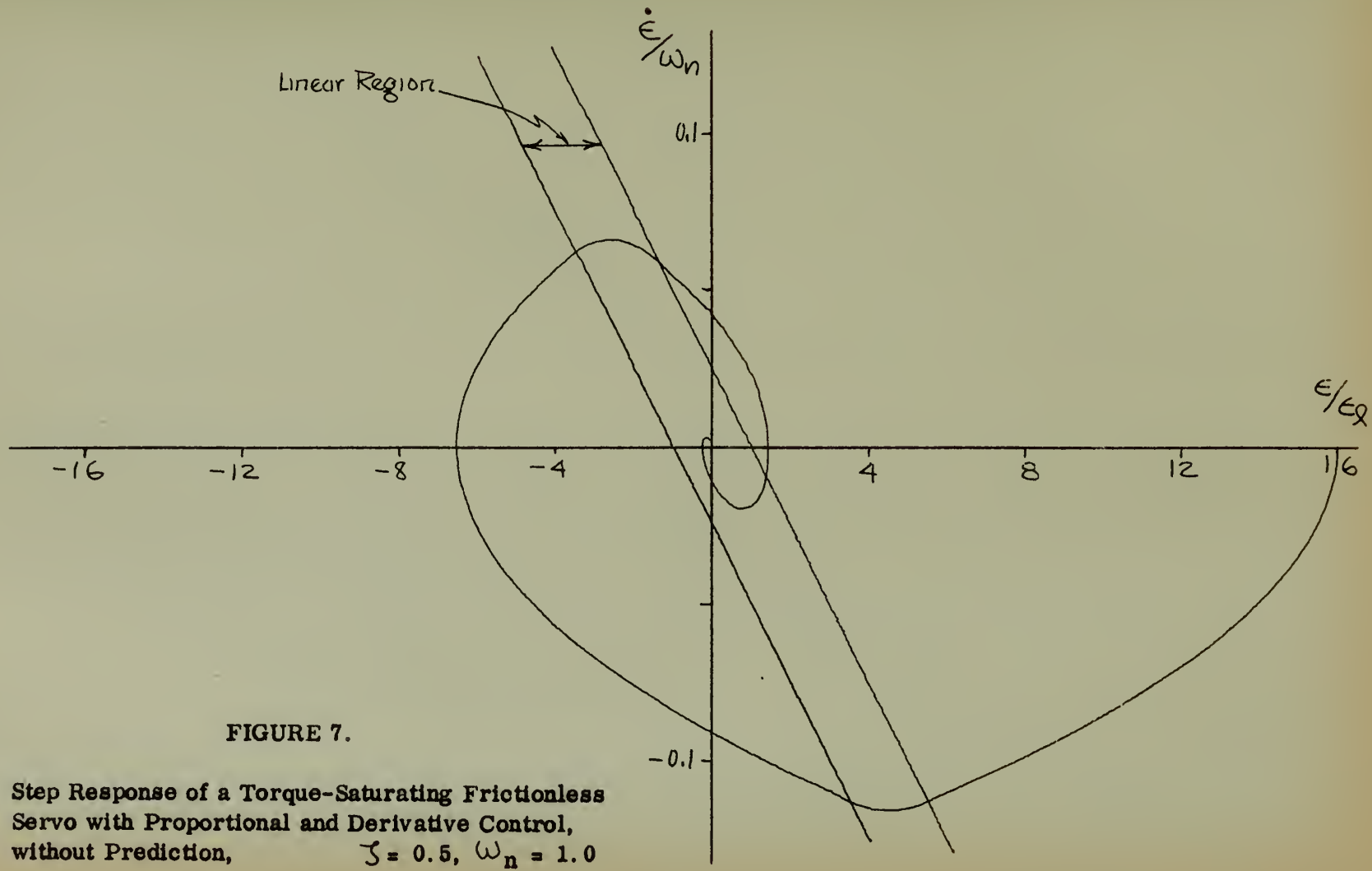

FIGURE 7.

Step Response of a Torque-Saturating Frictionless Servo with Proportional and Derivative Control, without Prediction, $\zeta = 0.5$, $\omega_n = 1.0$

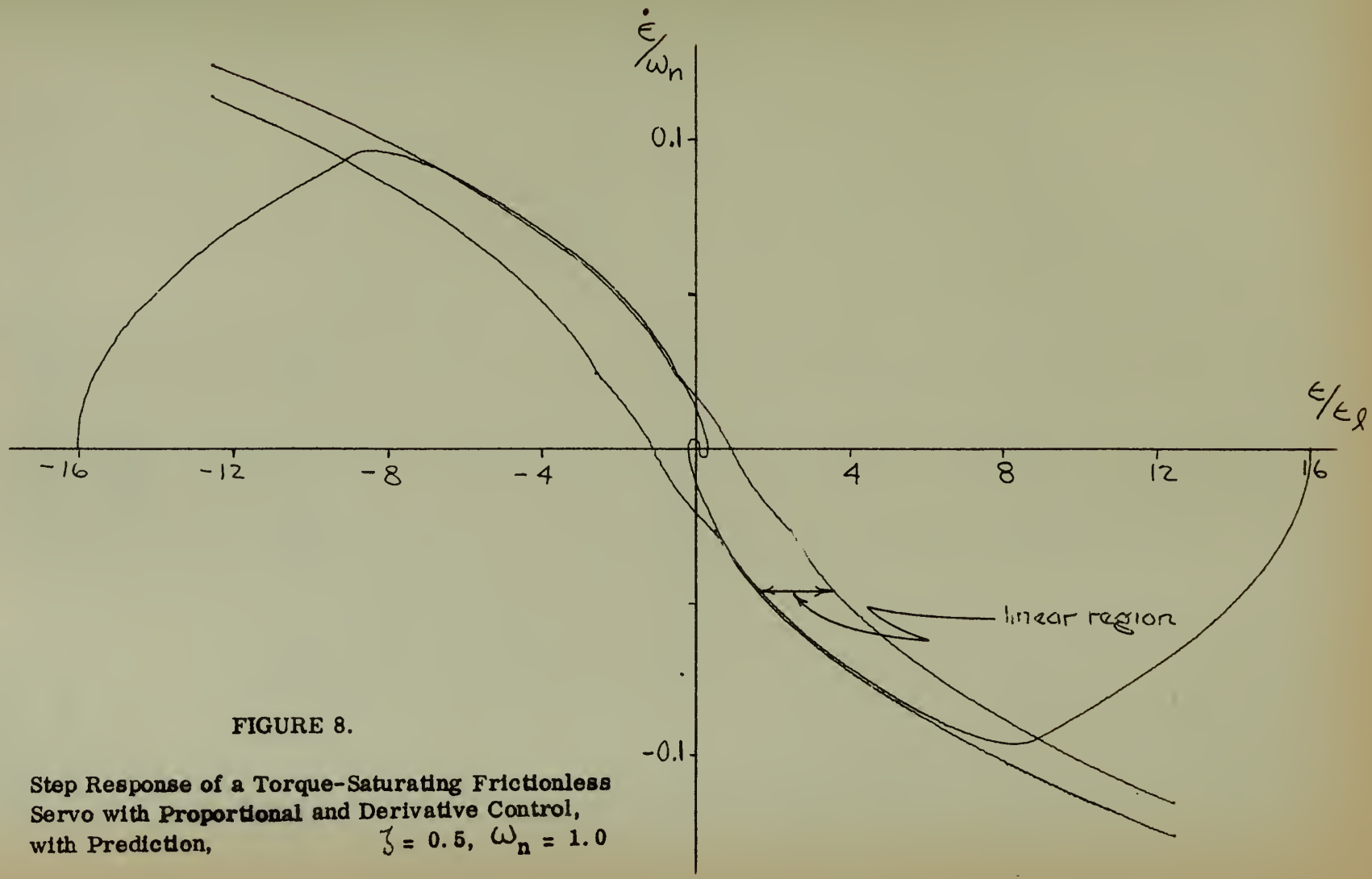

FIGURE 8.

Step Response of a Torque-Saturating Frictionless Servo with Proportional and Derivative Control, with Prediction, $\zeta = 0.5$, $\omega_n = 1.0$

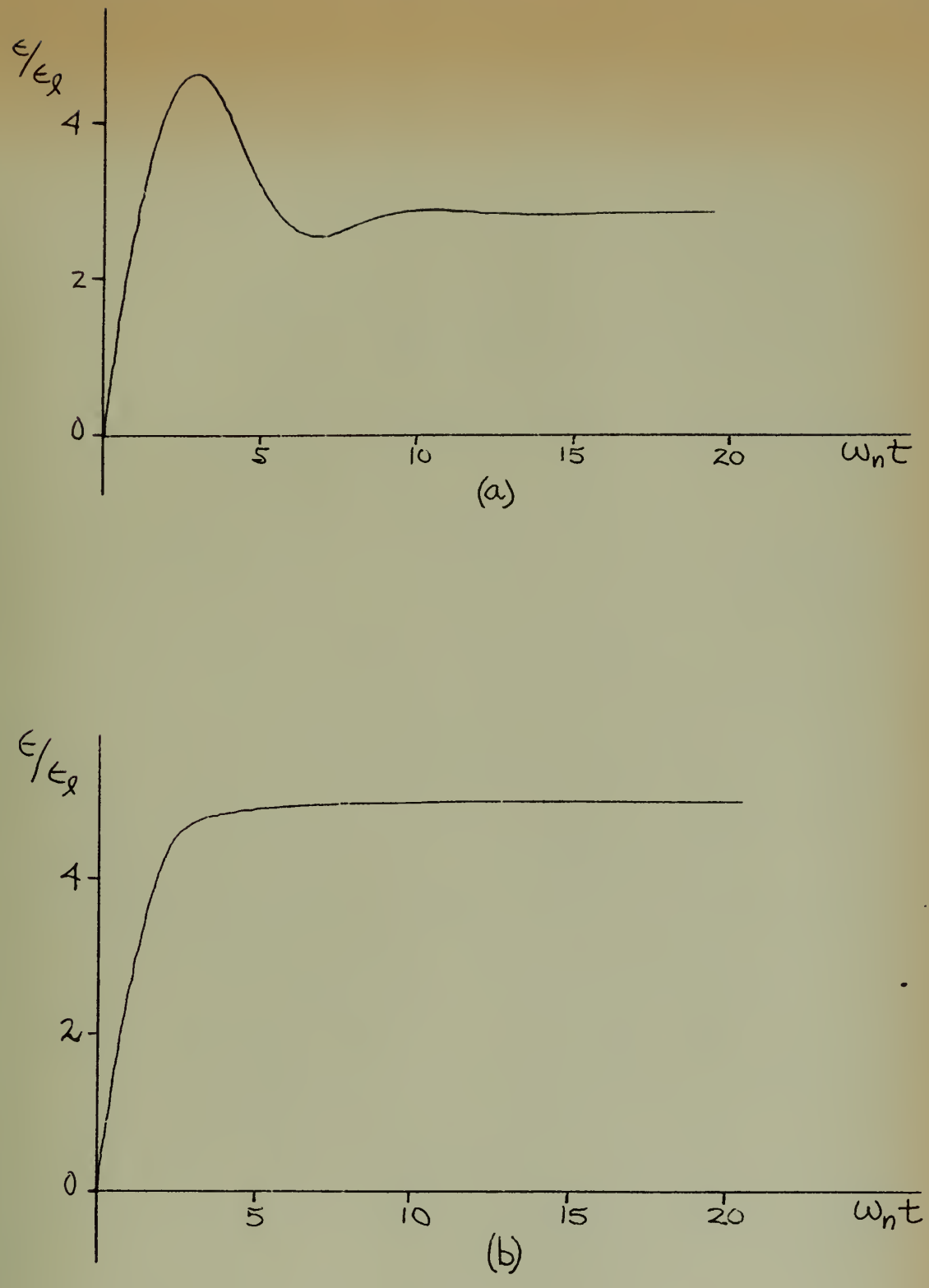

FIGURE 9.

Ramp Response of a Torque-Saturating Frictionless Servo with Proportional and Derivative Control,
$\zeta = 0.5$, $\omega_n = 1.0$, $\dot{\theta}_i/\omega_n = 0.07$
(a) Without Prediction **(b) With Prediction**

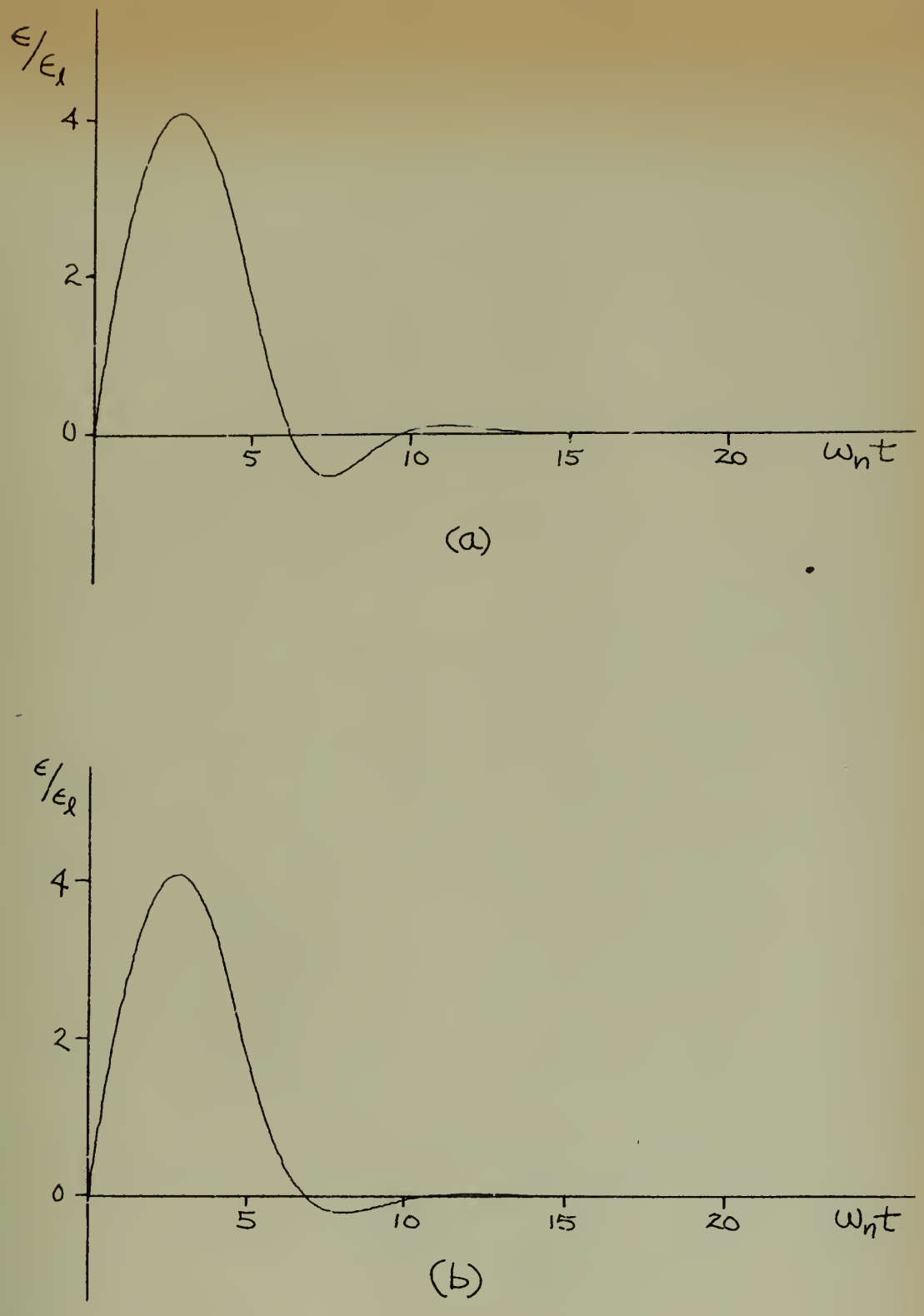

FIGURE 10.

Ramp Response of a Torque-Saturating Frictionless Servo with Proportional and Error Rate Control,
$\zeta = 0.5$, $\omega_n = 1.0$, $\dot{\theta}_i/\omega_n = 0.07$
(a) Without Prediction (b) With Prediction

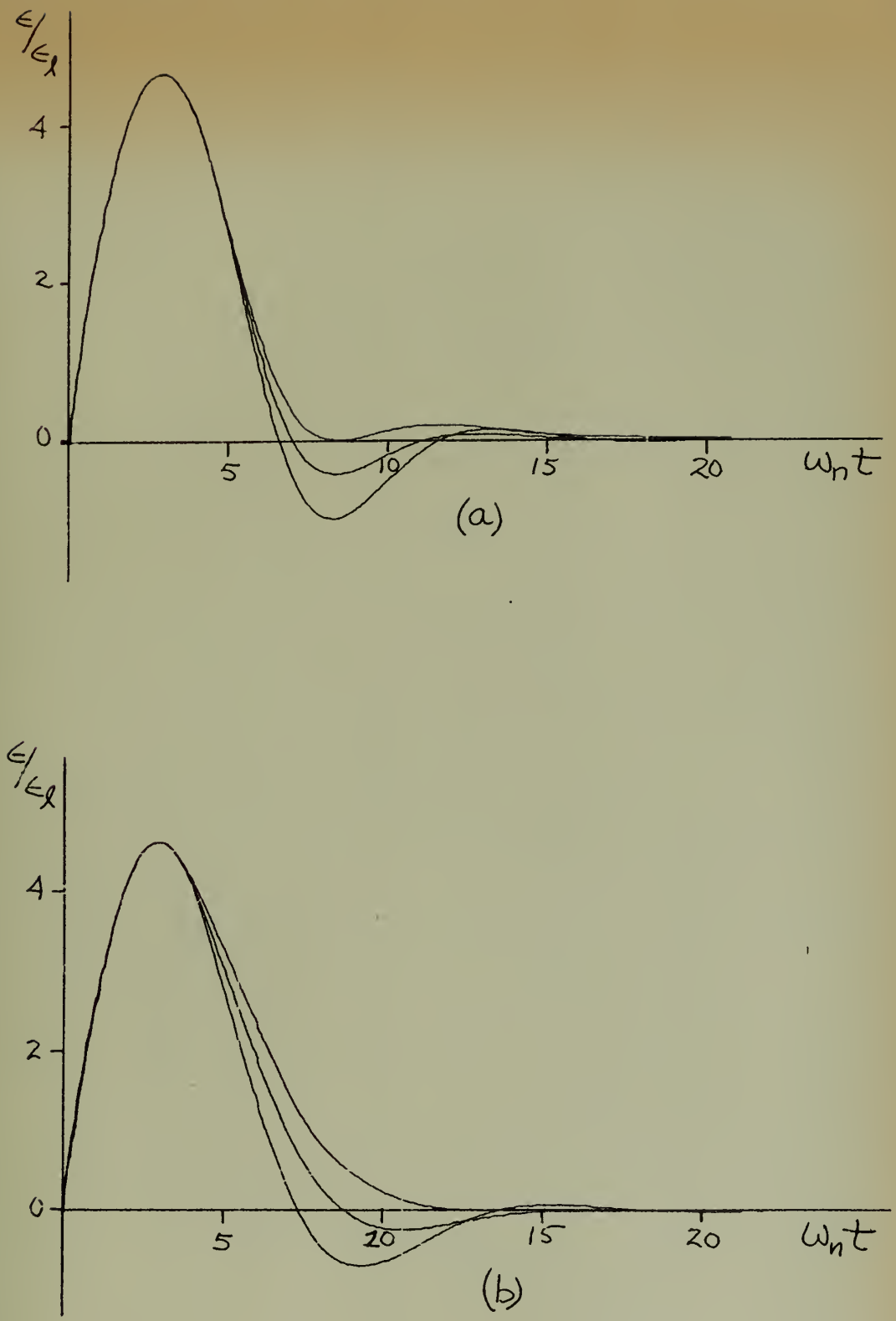

FIGURE 11.

Ramp Response of a Torque-Saturating Frictionless Servo with Proportional Control and Derivative Control through a High Pass Filter, $\zeta = 0.5$, $\omega_n = 1$, $\dot{\theta}_1/\omega_n = 0.07$. With High Pass Filter Cutoff Frequency $\omega_c = \omega_n/5$, $\omega_n/4$, $\omega_n/3$, Top to Bottom.
(a) Without Prediction (b) With Prediction

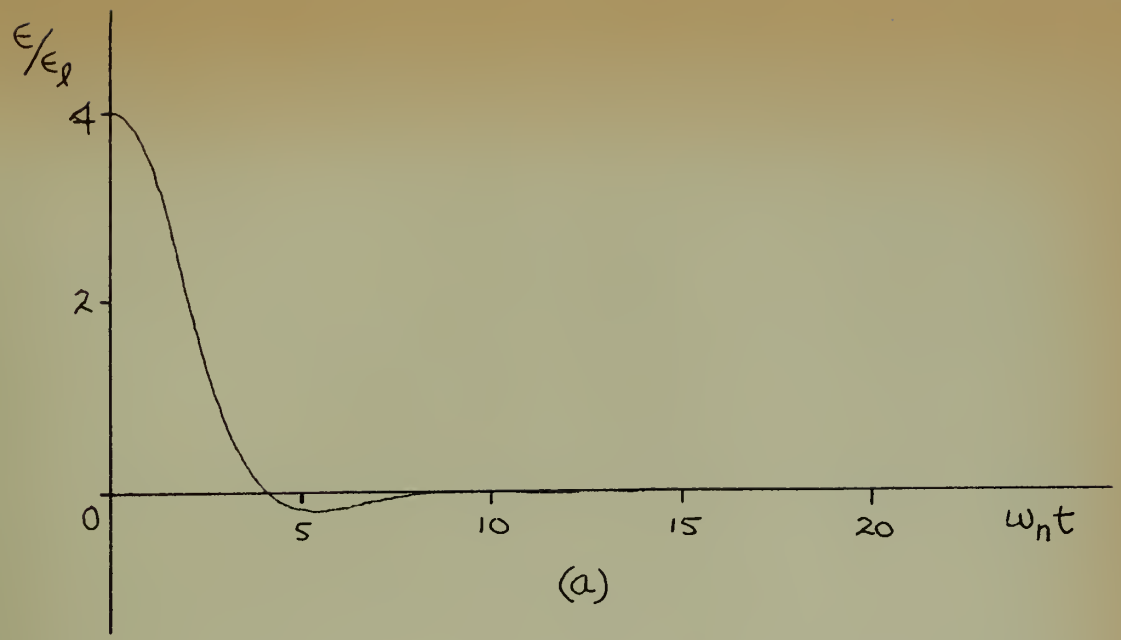

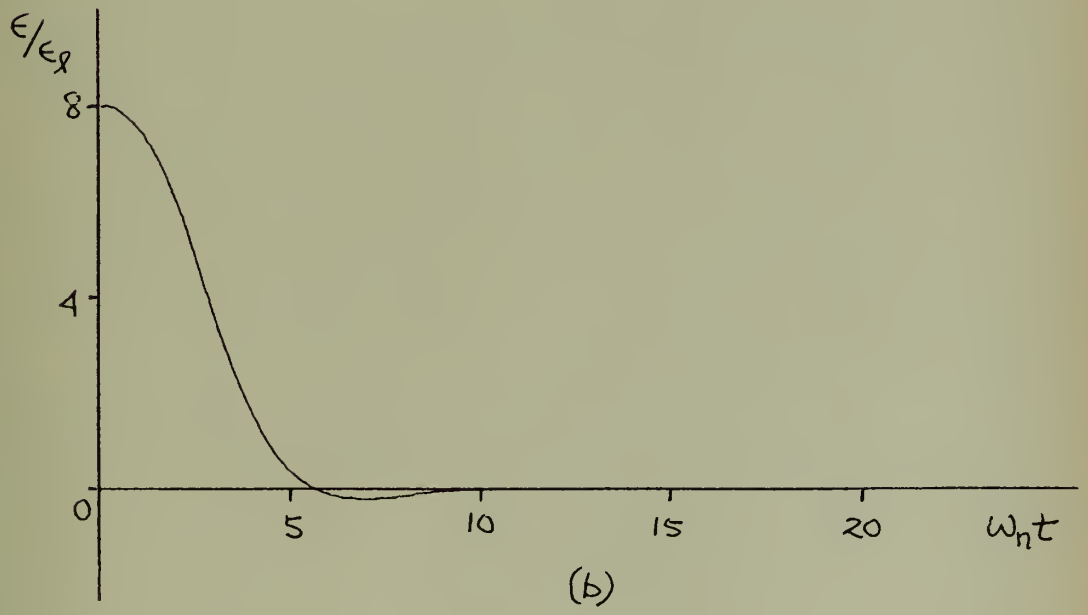

FIGURE 12.

Step Response of a Torque-Saturating Frictionless Servo with Proportional Control, Derivative Control, and THYRITE for Prediction, $\zeta = 0.5$, $\omega_n = 1.0$

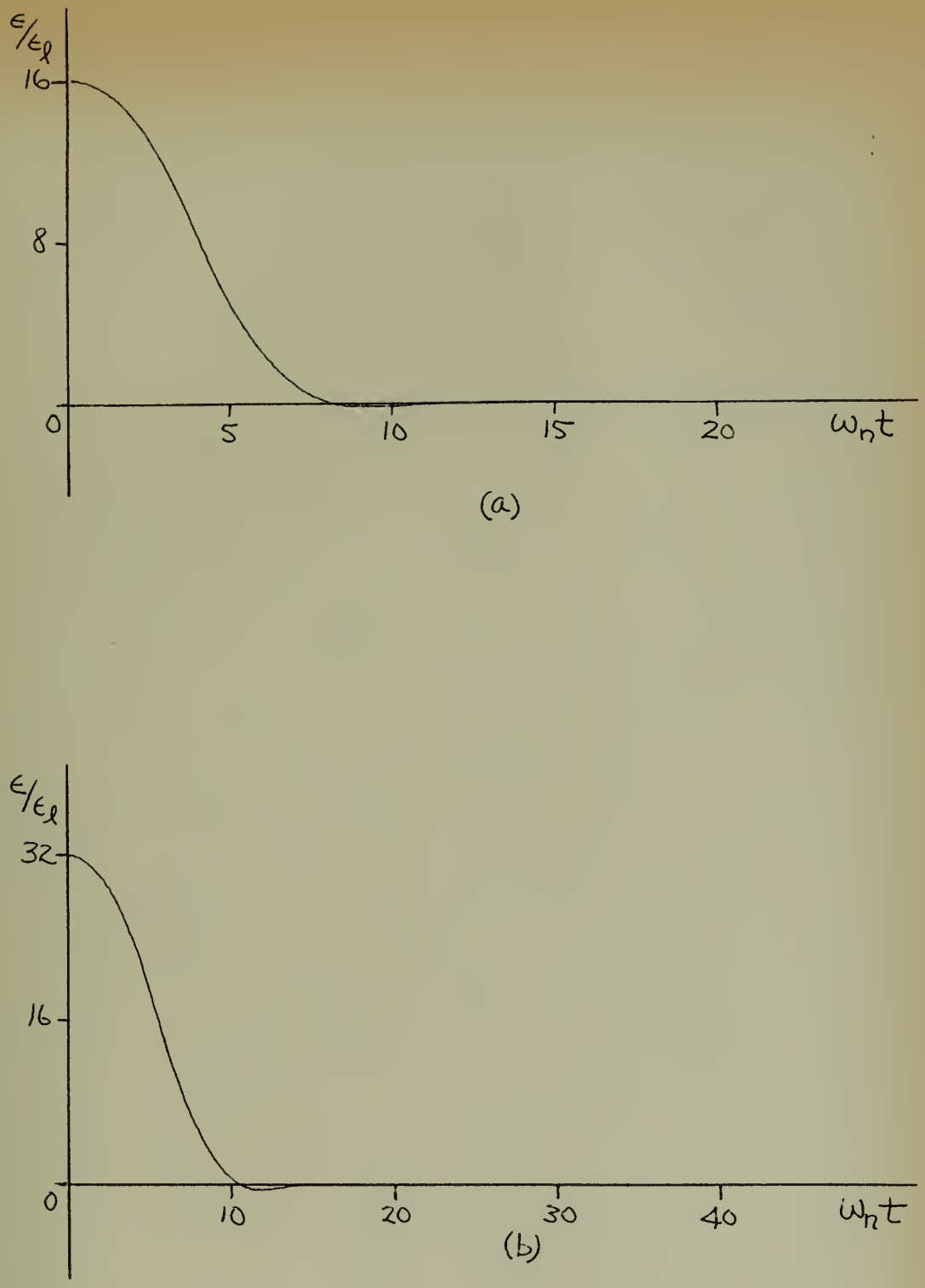

FIGURE 13

Step Response of a Torque-Saturating Frictionless Servo with Proportional Control, Derivative Control, and THYRITE for Prediction, $\zeta = 0.5$, $\omega_n = 1.0$

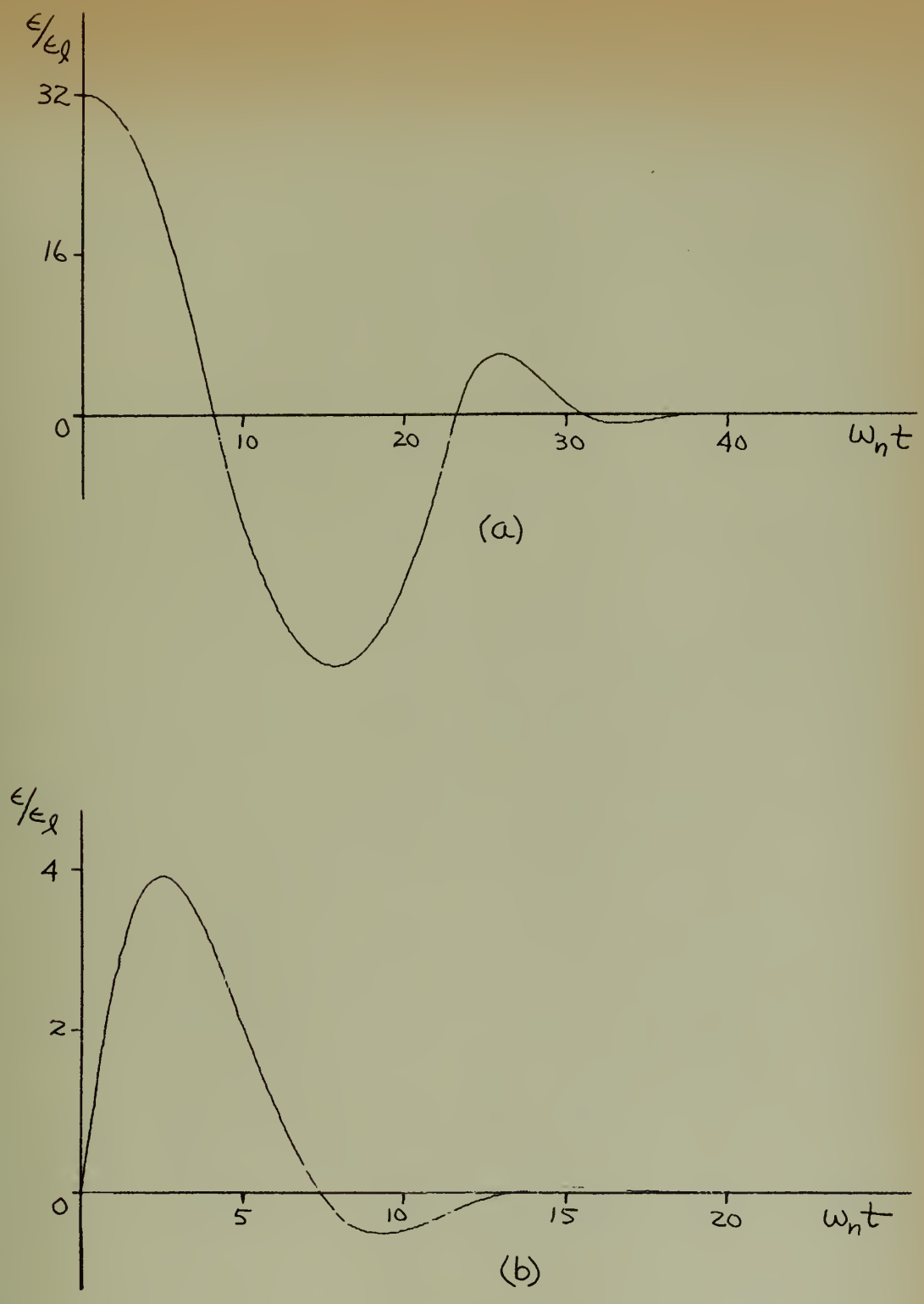

FIGURE 14.

Response of a Torque-Saturating Frictionless Servo with Proportional Control, Derivative Control Through a High Pass Filter, and THYRITE for Prediction, $J = 0.5$, $\omega_n = 1.0$, $\omega_c = \omega_n/3$
(a) Step Input, $\epsilon/\epsilon_\ell = 32$ (b) Ramp Input, $\dot{\theta}_i/\omega_n = .07$

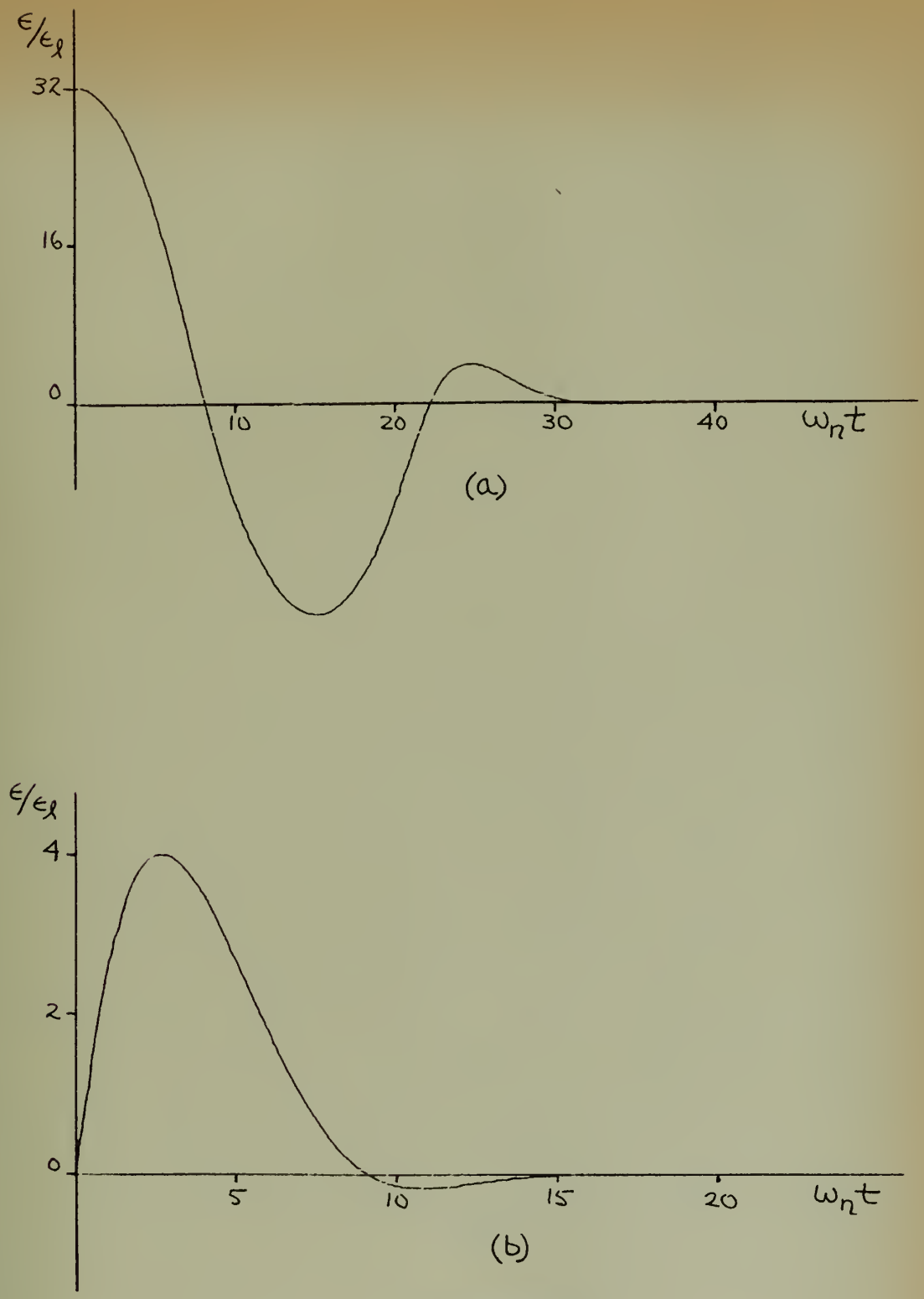

FIGURE 15.

Response of a Torque-Saturating Frictionless Servo with Proportional Control, Derivative Control Through a High Pass Filter, and THYRITE for Prediction, $\omega_c = \omega_n/4$, $\zeta = 0.5$, $\omega_n = 1.0$
(a) Step Input, $\epsilon/\epsilon_\ell = 32$ (b) Ramp Input, $\dot{\theta}_i/\omega_n = 0.07$

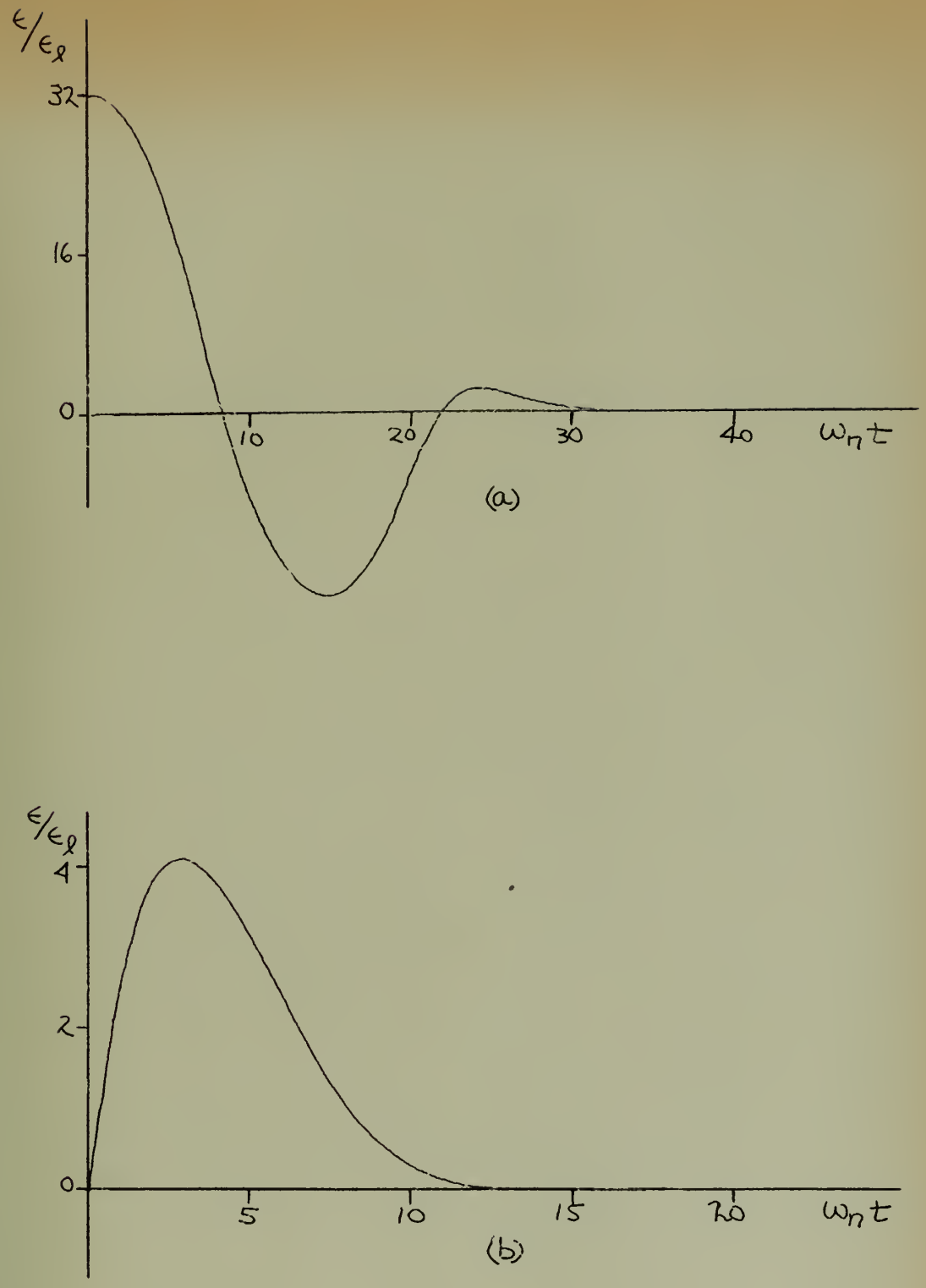

FIGURE 16.

Response of a Torque-Saturating Frictionless Servo with Proportional Control, Derivative Control Through a High Pass Filter, and THYRITE for Prediction, $\omega_c = \omega_n/5$, $\zeta = 0.5$, $\omega_n = 1.0$.
(a) Step Input, $\epsilon/\epsilon_\ell = 32$ (b) Ramp Input, $\dot{\theta}_i/\omega_n = .07$

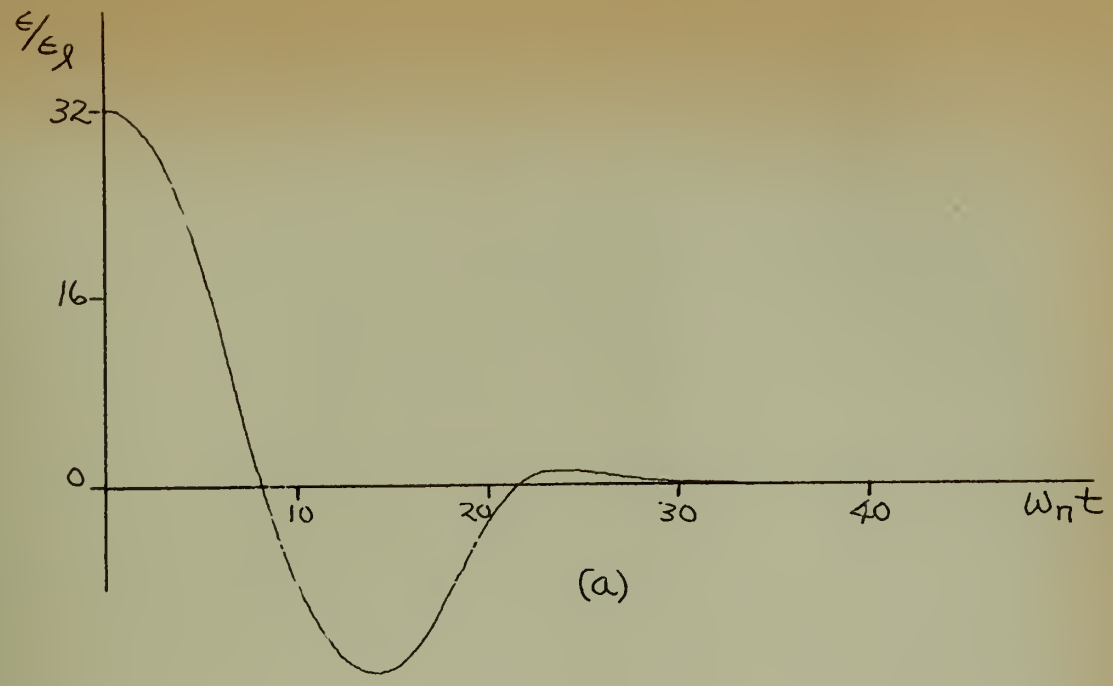

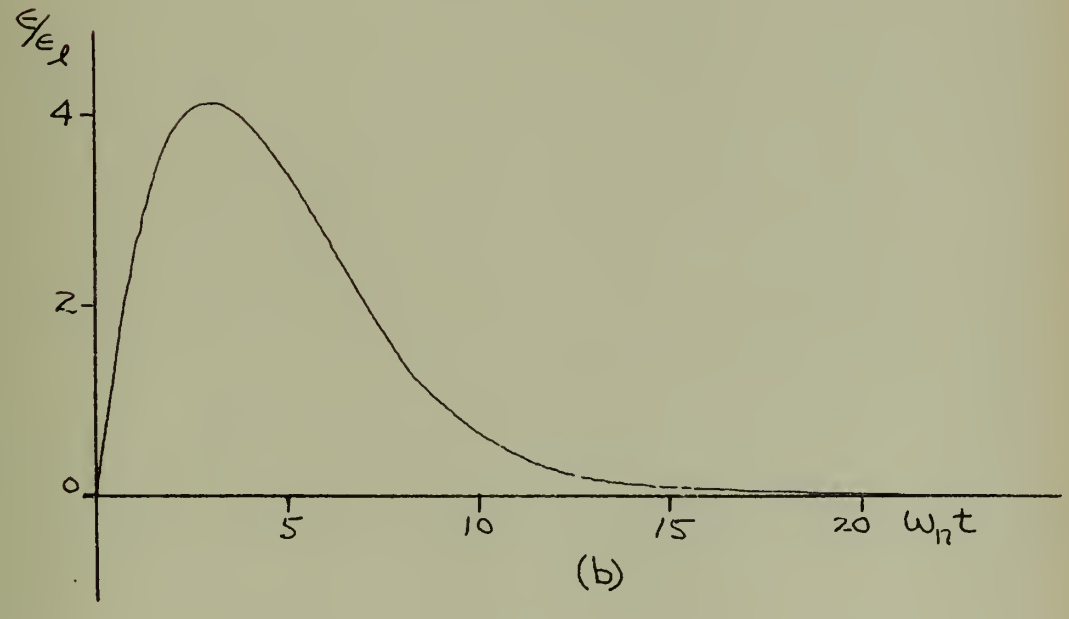

FIGURE 17.

Response of a Torque-Saturating Frictionless Servo with Proportional Control, Derivative Control Through A High Pass Filter, and THYRITE for Prediction, $\omega_c = \omega_n/6$, $\zeta = 0.5$, $\omega_n = 1.0$.
(a) Step Input, $\epsilon/\epsilon_\ell = 32$ (b) Ramp Input, $\dot{\theta}_i/\omega_n = .07$

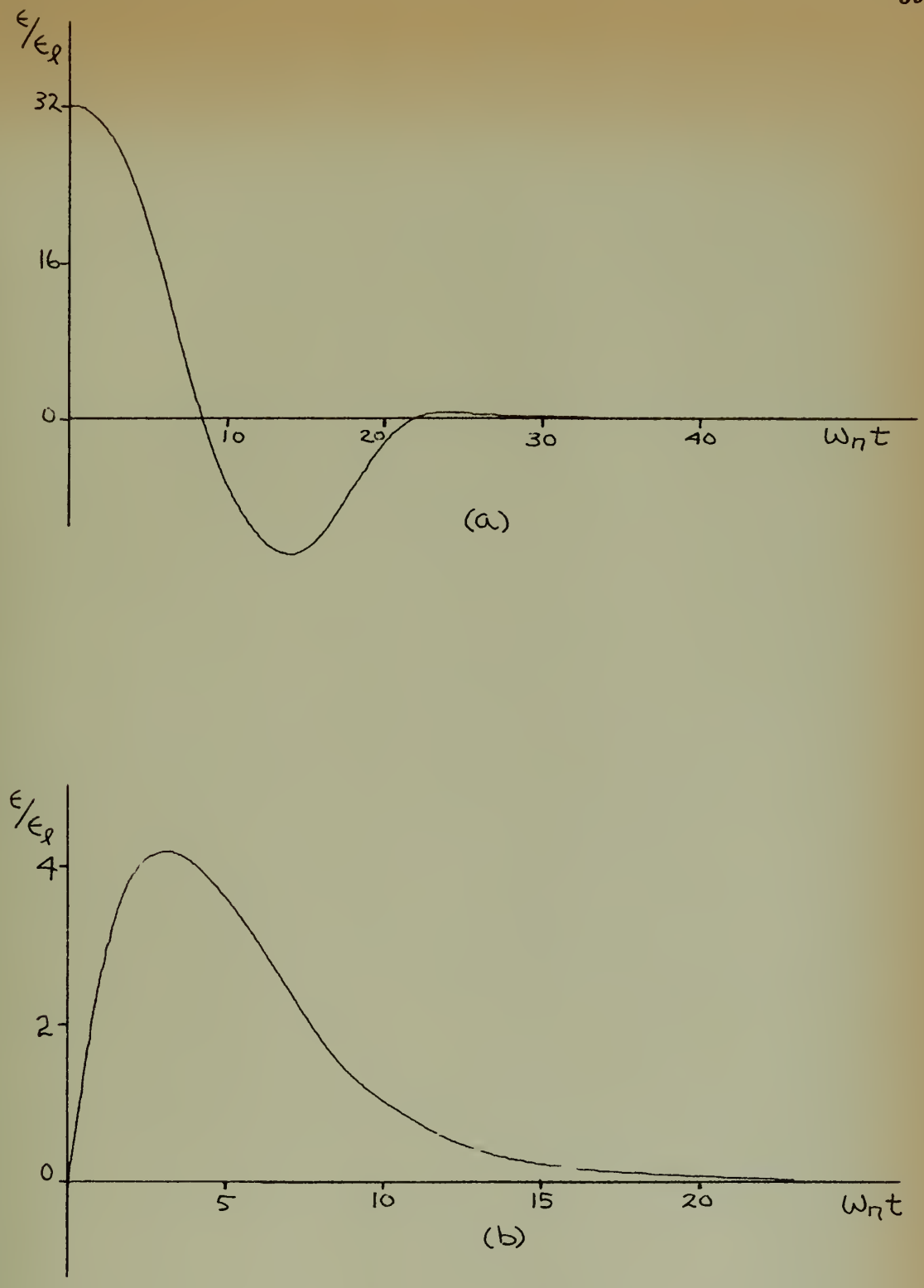

FIGURE 18.

Response of a Torque-Saturating Frictionless Servo with Proportional Control, Derivative Control Through a High Pass Filter, and THYRITE for Prediction, $\omega_c = \omega_n/7$, $\zeta = 0.5$, $\omega_n = 1.0$.
(a) Step Input, $\epsilon/\epsilon_\ell = 32$ (b) Ramp Input, $\dot{\theta}_i/\omega_n = .07$

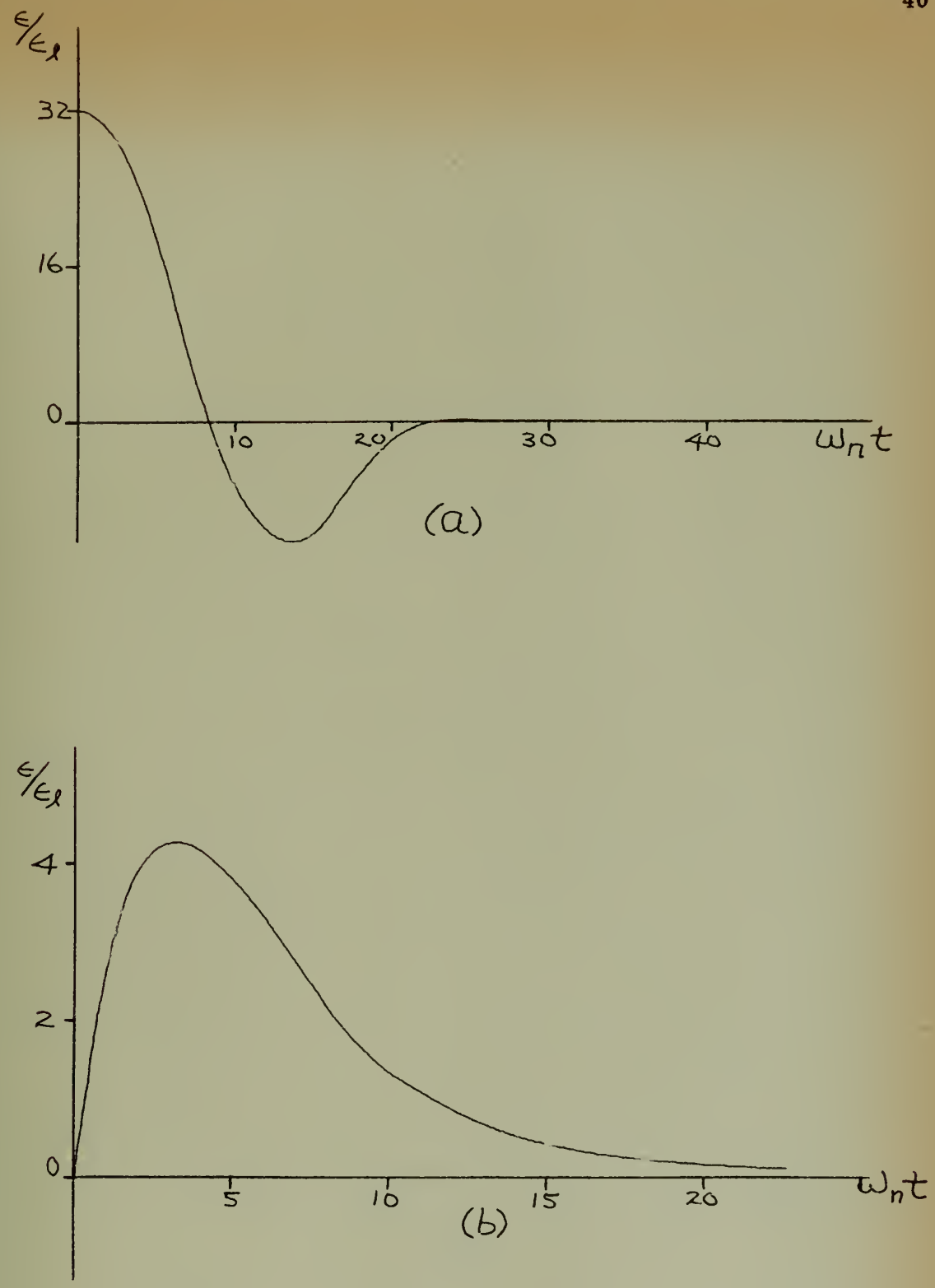

FIGURE 19.

Response of a Torque-Saturating Frictionless Servo with Proportional Control, Derivative Control Through a High Pass Filter, and THYRITE for Prediction, $\omega_c = \omega_n/8$, $\mathcal{J} = 0.5$, $\omega_n = 1.0$.
(a) Step Input, $\epsilon/\epsilon_\ell = 32$ (b) Ramp Input, $\dot{\theta}_i/\omega_n = .07$

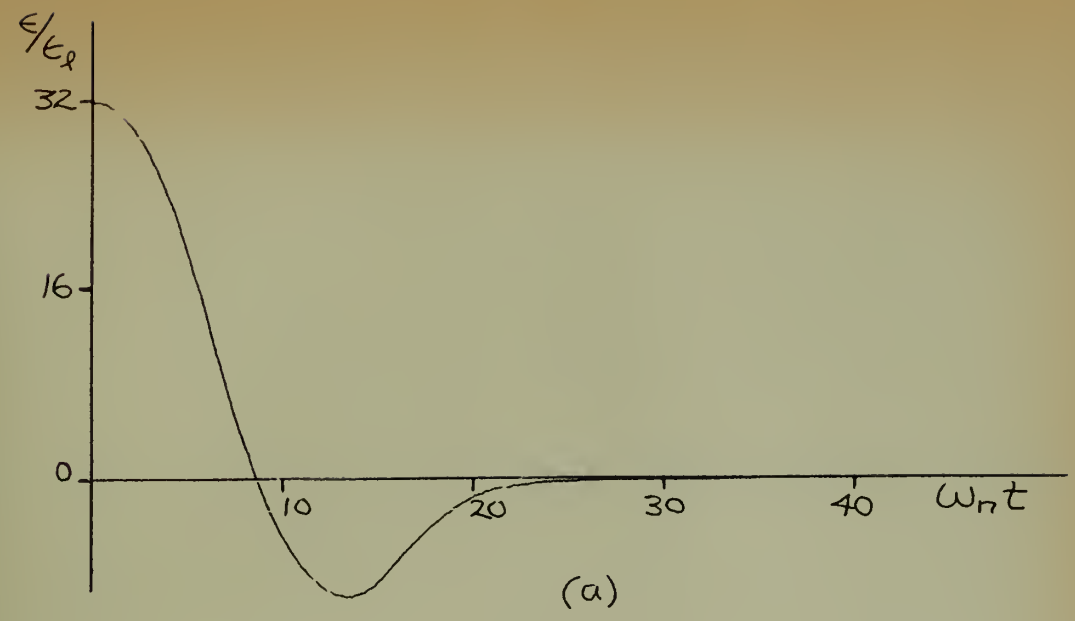

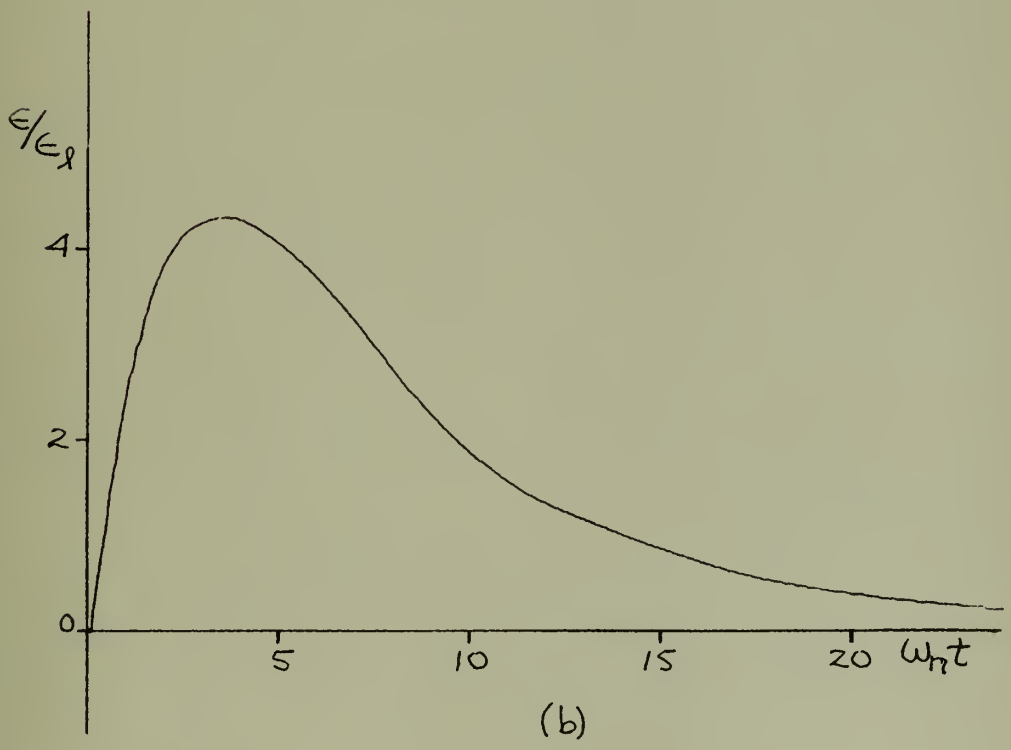

FIGURE 20.

Response of a Torque-Saturating Frictionless Servo with Proportional Control, Derivative Control Through a High Pass Filter, and THYRITE for Prediction, $\omega_c = \omega_n/10$, $\mathcal{J} = 0.5$, $\omega_n = 1.0$.
(a) Step Input, $\epsilon/\epsilon_\ell = 32$ (b) Ramp Input, $\dot{\theta}_i/\omega_n = .07$

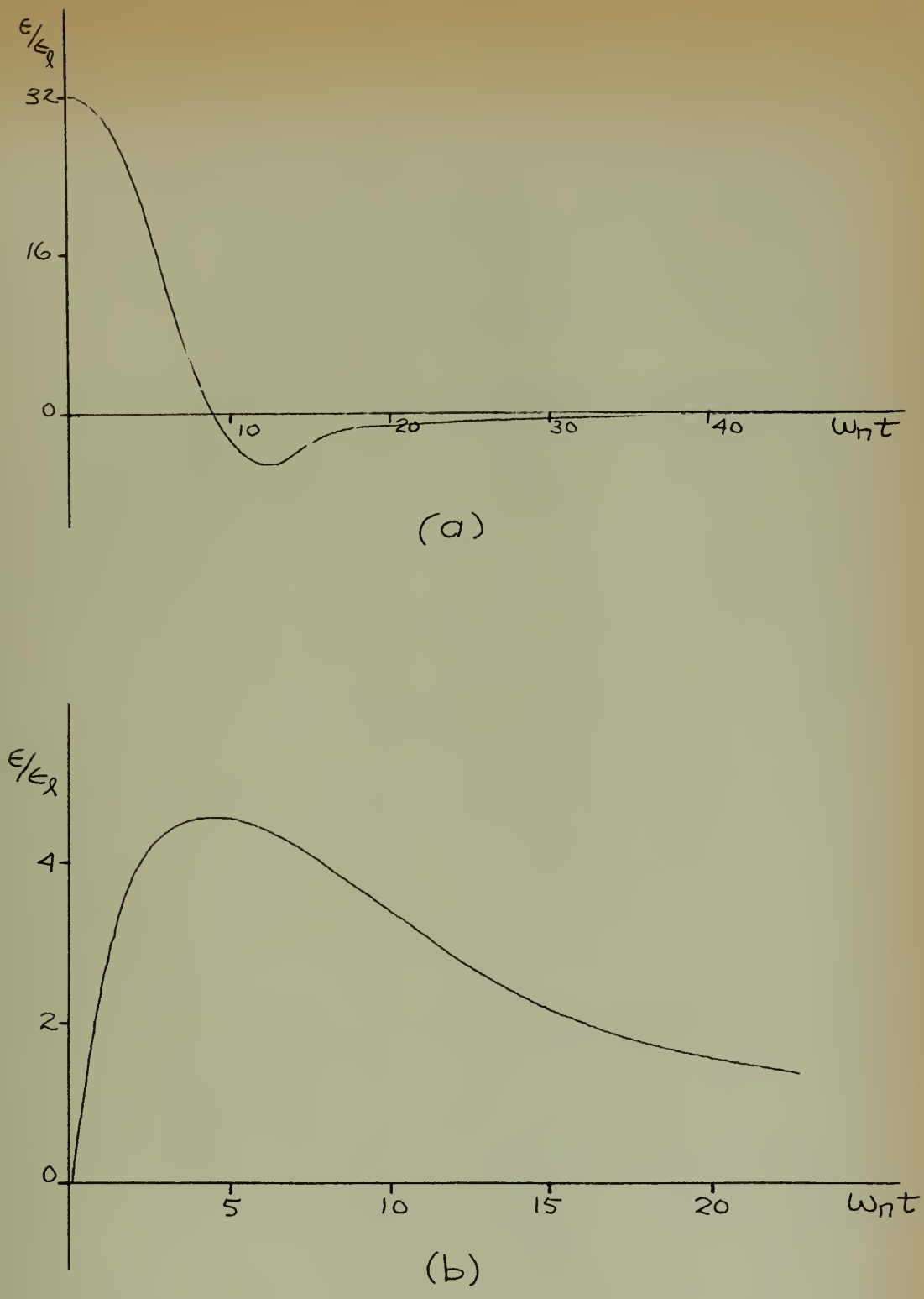

FIGURE 21

Response of a Torque-Saturating Frictionless Servo with Proportional Control, Derivative Control Through a High Pass Filter, and THYRITE for Prediction, $\omega_c = \omega_n/20$, $\zeta = 0.5$, $\omega_n = 1.0$.
(a) Step Input, $\epsilon/\epsilon_\ell = 32$ (b) Ramp Input, $\dot{\theta}_i/\omega_n = .07$

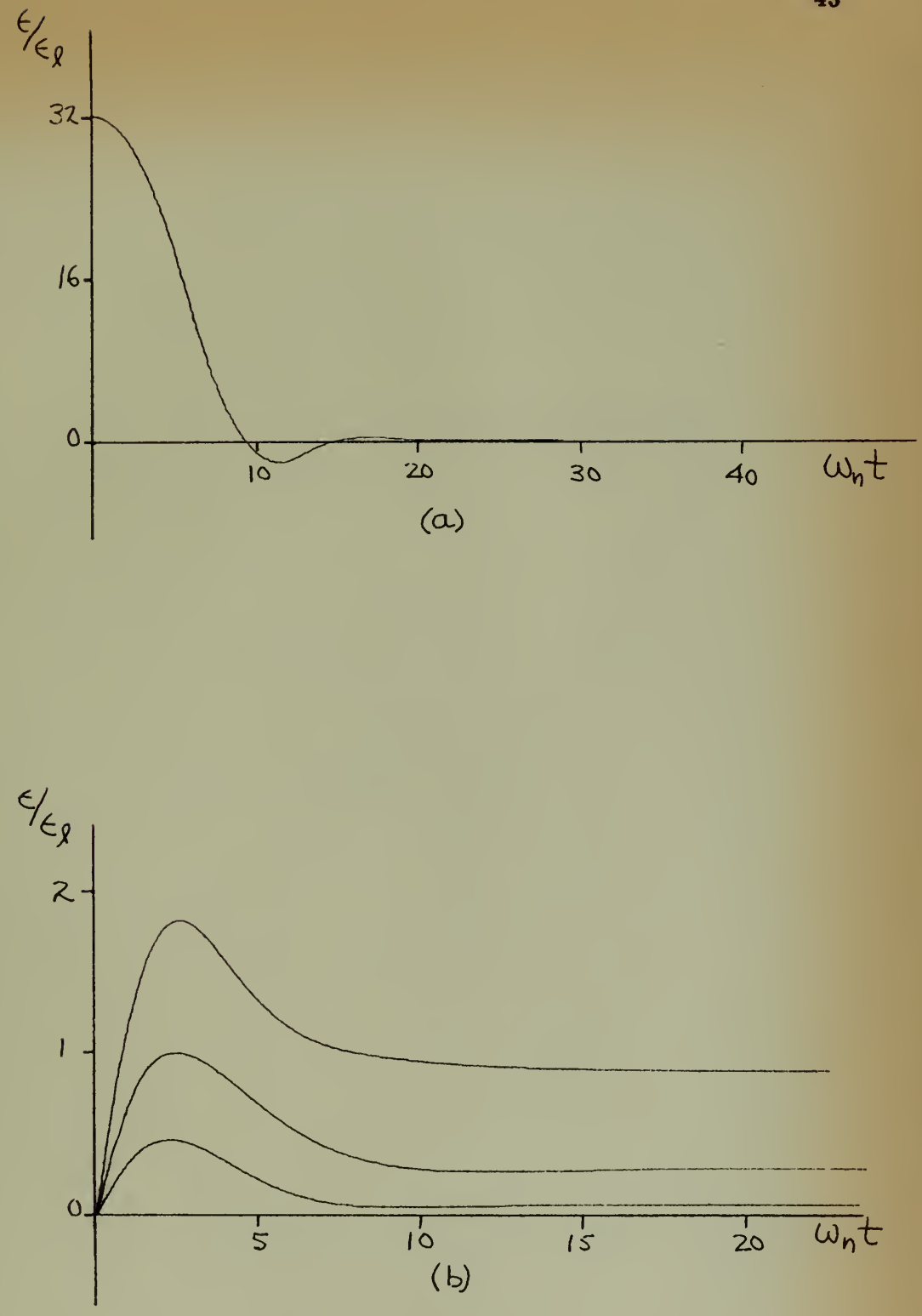

FIGURE 22.

Response of a Torque-Saturating Frictionless Servo with Proportional Control, Derivative Control, and Prediction, plus a High Pass Filter on Derivative Feedback. $\omega_c = \omega_n/3$.
(a) Step Input, $\epsilon/\epsilon_i = 32$
(b) Ramp Input, $\dot{\theta}_i/\omega_n = 0.035$, 0.02, and 0.01 from Top to Bottom.

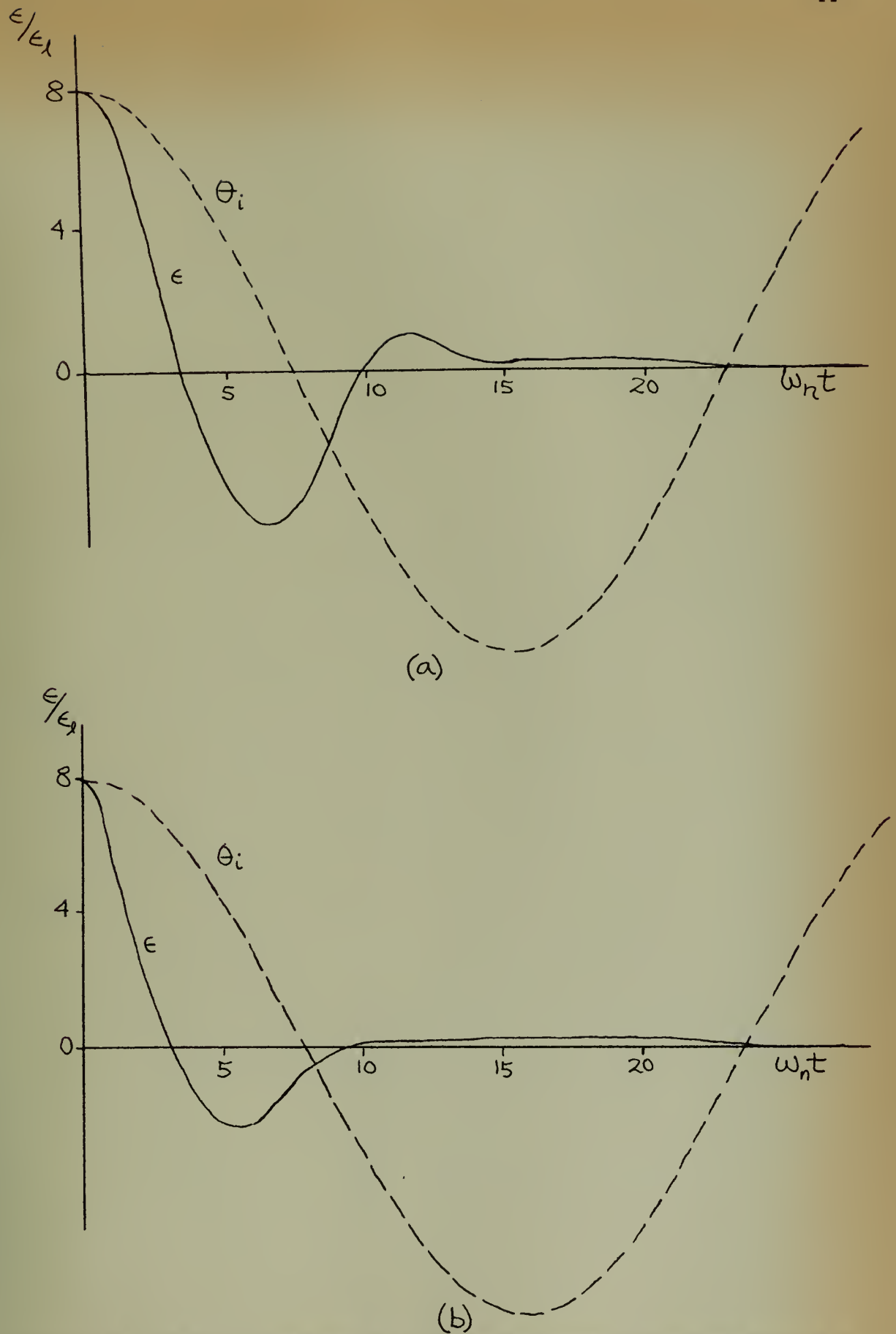

FIGURE 23. Sine Wave Response of a Torque-Saturating Frictionless Servo with Proportional and Derivative Control, $\mathcal{J} = 0.5$, $\omega_n = 1.0$, $\Omega/\omega_n = 1/5$
(a) Without Prediction (b) With Prediction

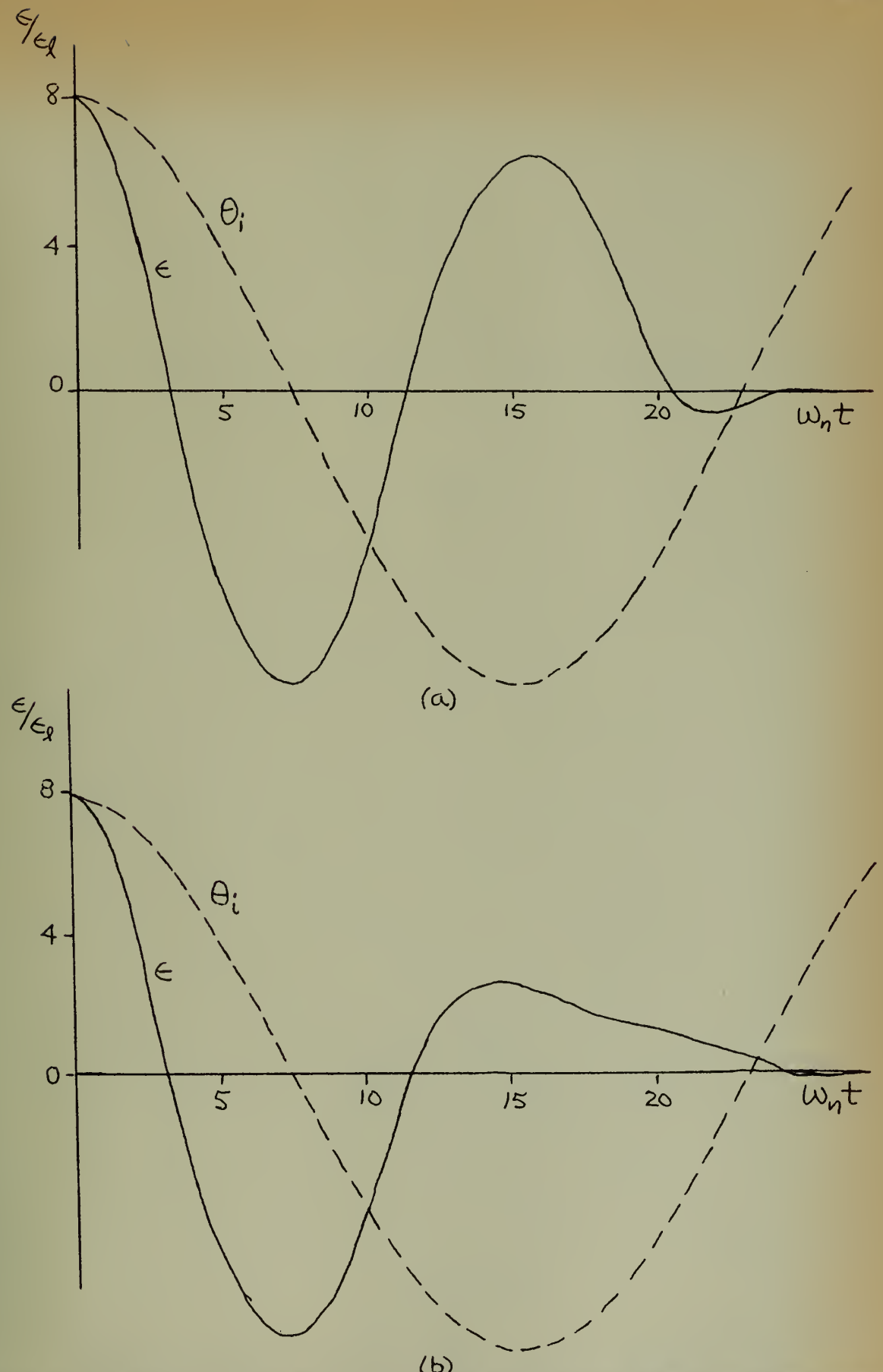

FIGURE 24. Sine Wave Response of a TSFS with Proportional Control and Derivative Control through a High Pass Filter. $\mathcal{J} = 0.5$, $\omega_n = 1.0$, $\omega_c = \omega_n/3$, $\Omega/\omega_n = 1/5$
(a) Without Prediction (b) With Prediction

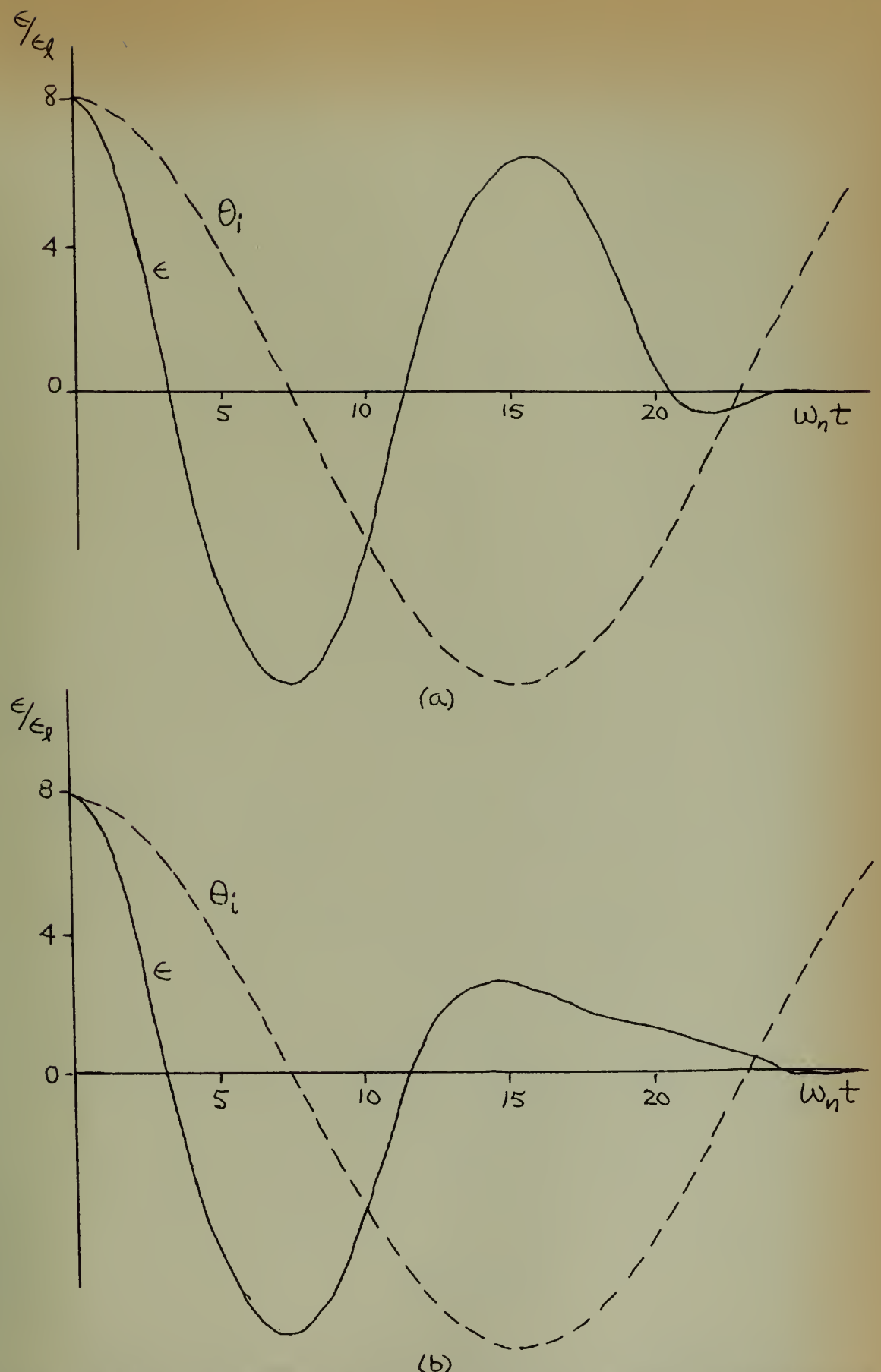

FIGURE 24. Sine Wave Response of a TSFS with Proportional Control and Derivative Control through a High Pass Filter. $\zeta = 0.5$, $\omega_n = 1.0$, $\omega_c = \omega_n/3$, $\Omega/\omega_n = 1/5$
(a) Without Prediction (b) With Prediction

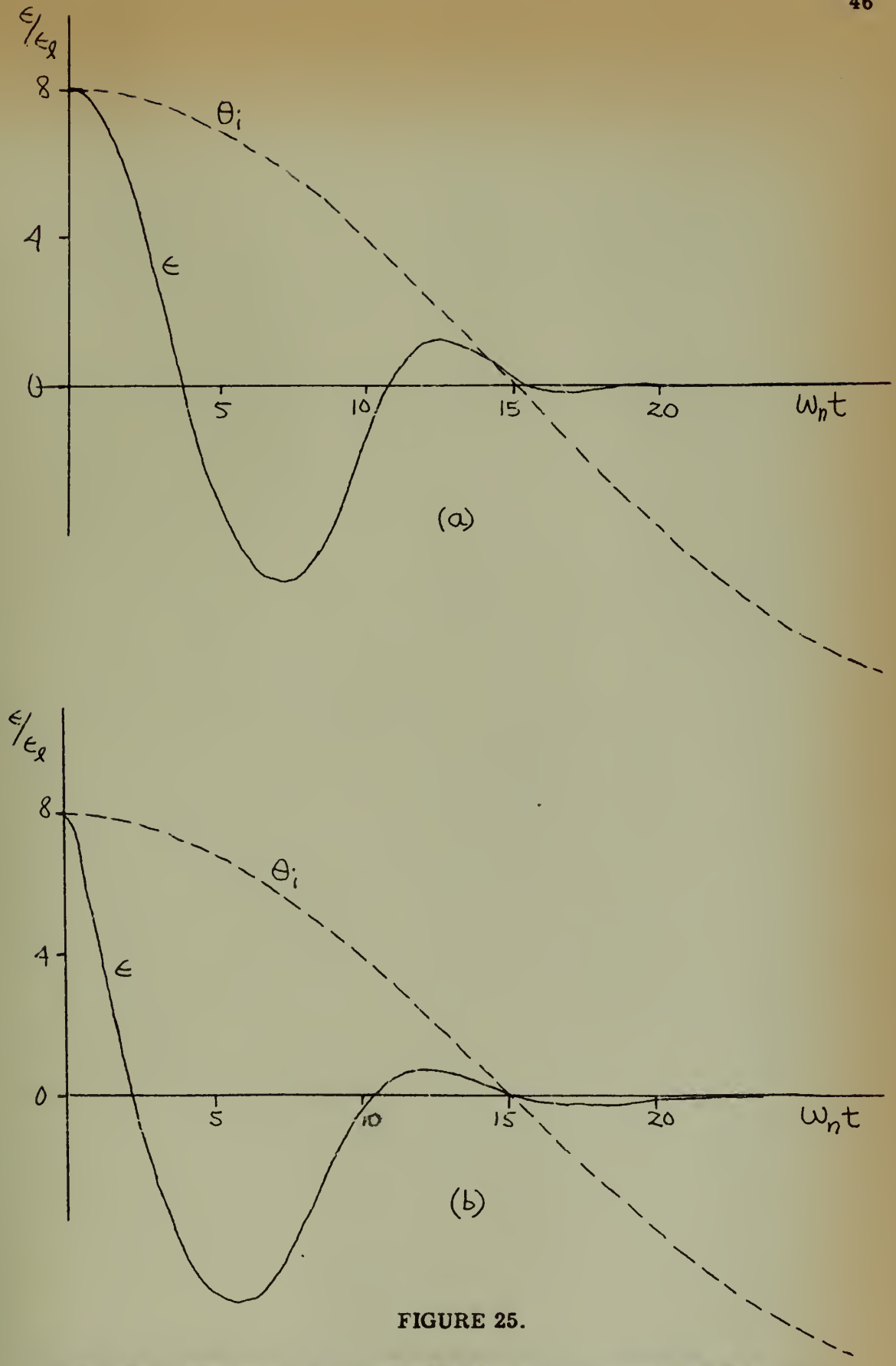

FIGURE 25.

Sine Wave Response of a Torque-Saturating Frictionless Servo with Proportional Control and Derivative Control through a High Pass Filter.
$\mathcal{J} = 0.5, \omega_n = 1.0, \omega_c = \omega_n/3, \Omega/\omega_n = 0.1$
(a) Without Prediction **(b) With Prediction**

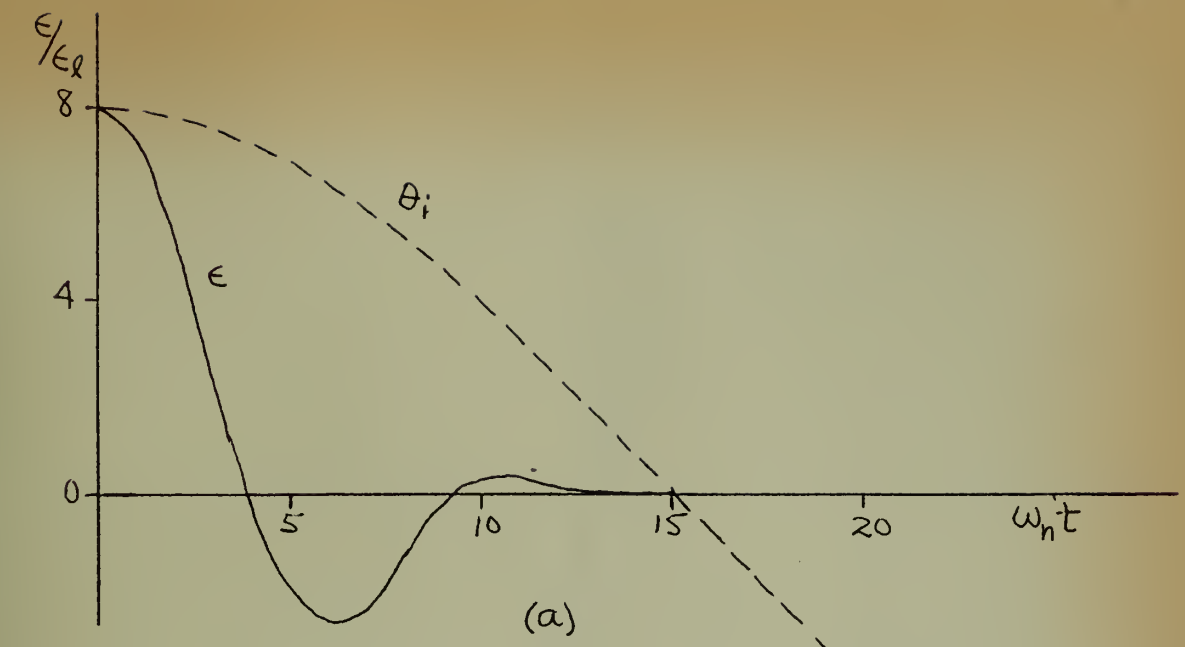

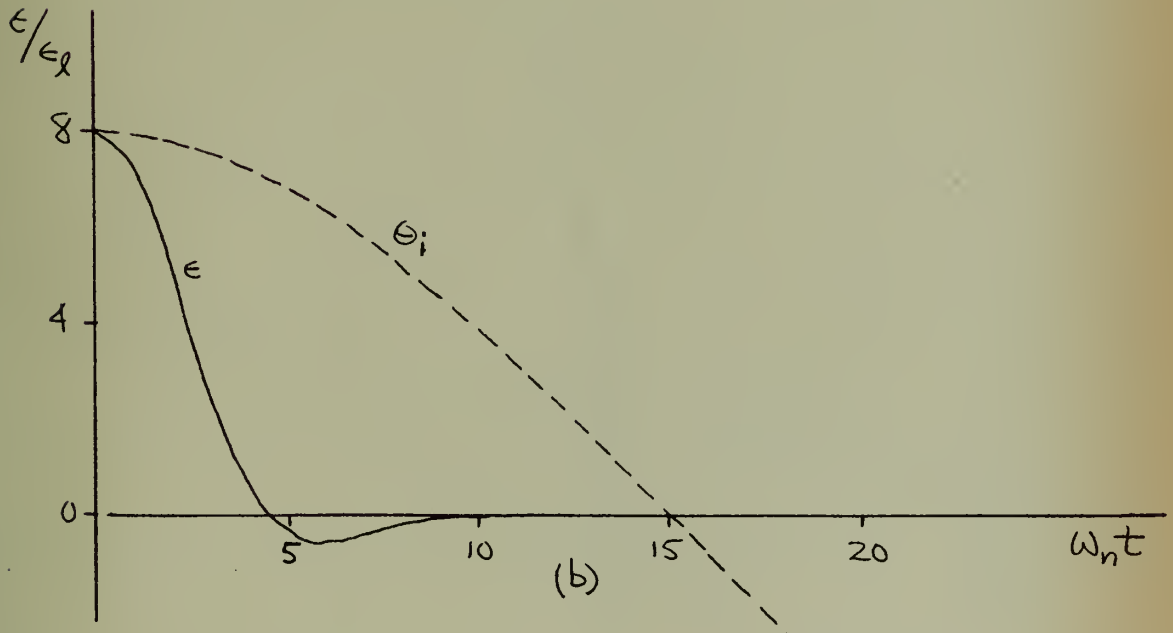

FIGURE 26.

Sine Wave Response of a Torque-Saturating Frictionless Servo with Proportional and Derivative Control, $\zeta = 0.5, \omega_n = 1.0, \Omega/\omega_n = 0.1$
(a) Without Prediction **(b) With Prediction**

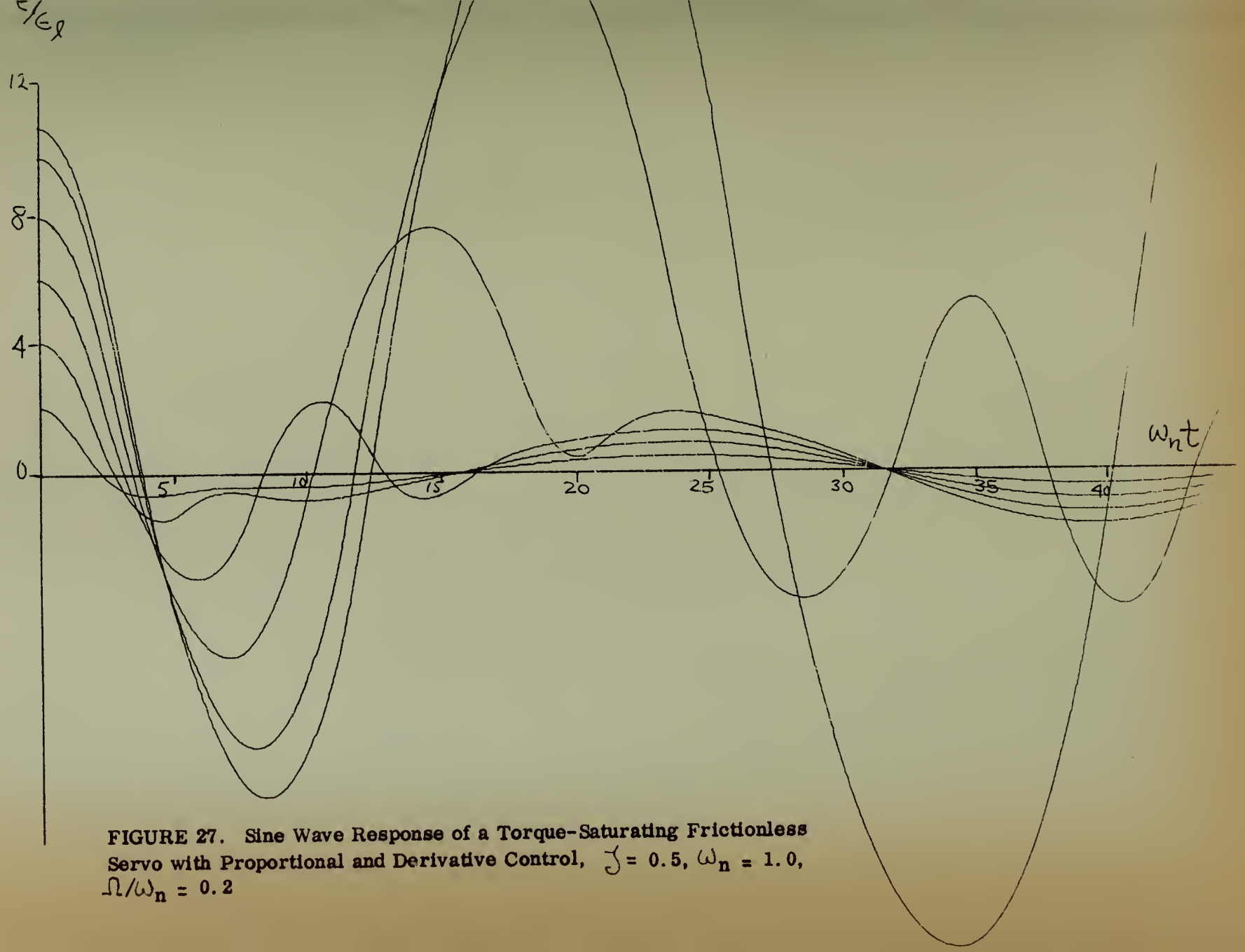

FIGURE 27. Sine Wave Response of a Torque-Saturating Frictionless Servo with Proportional and Derivative Control, $\zeta = 0.5$, $\omega_n = 1.0$, $\Omega/\omega_n = 0.2$

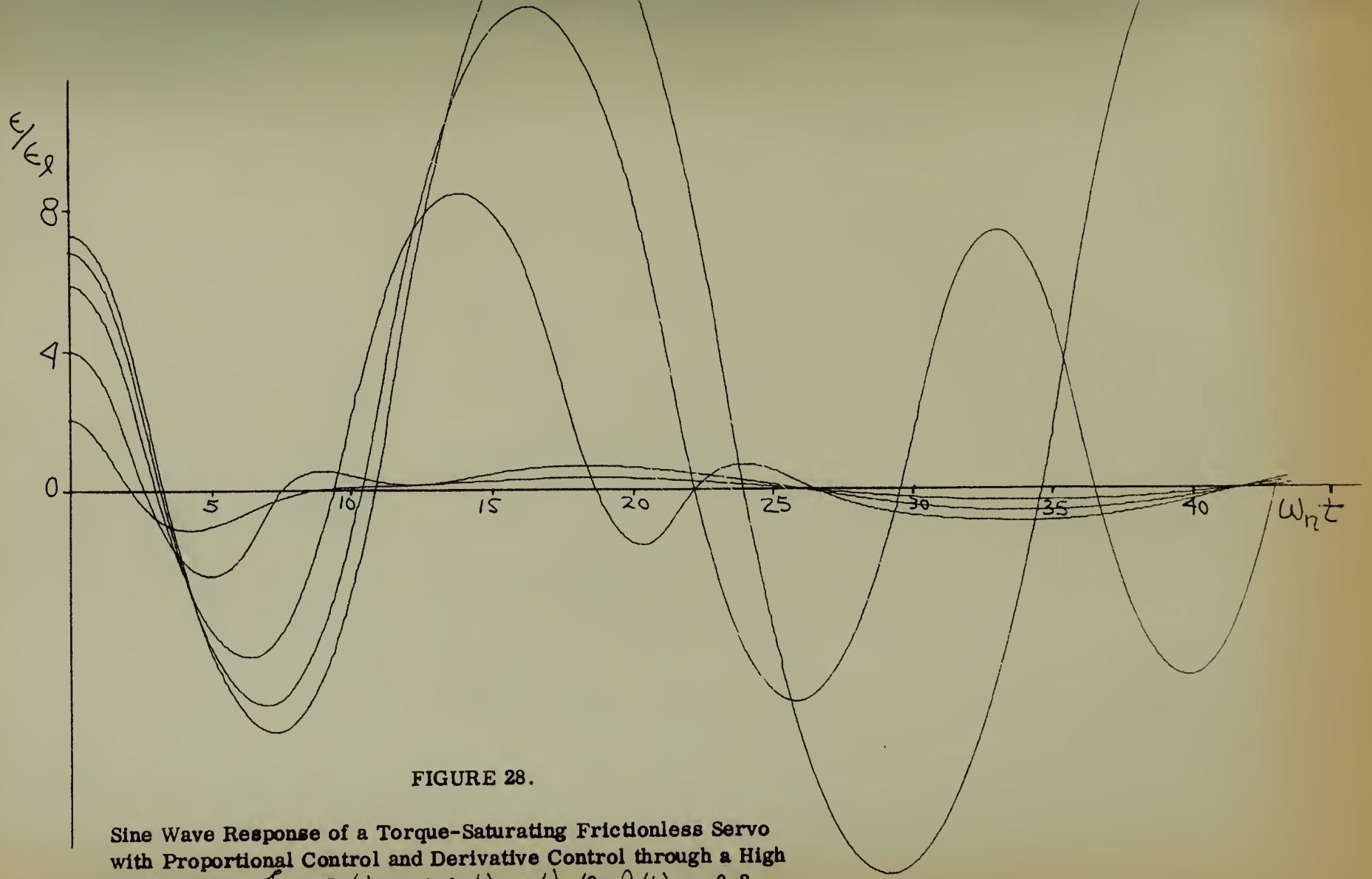

FIGURE 28.

Sine Wave Response of a Torque-Saturating Frictionless Servo with Proportional Control and Derivative Control through a High Pass Filter, $\zeta = 0.5$, $\omega_n = 1.0$, $\omega_c = \omega_n/3$, $\Omega/\omega_n = 0.2$

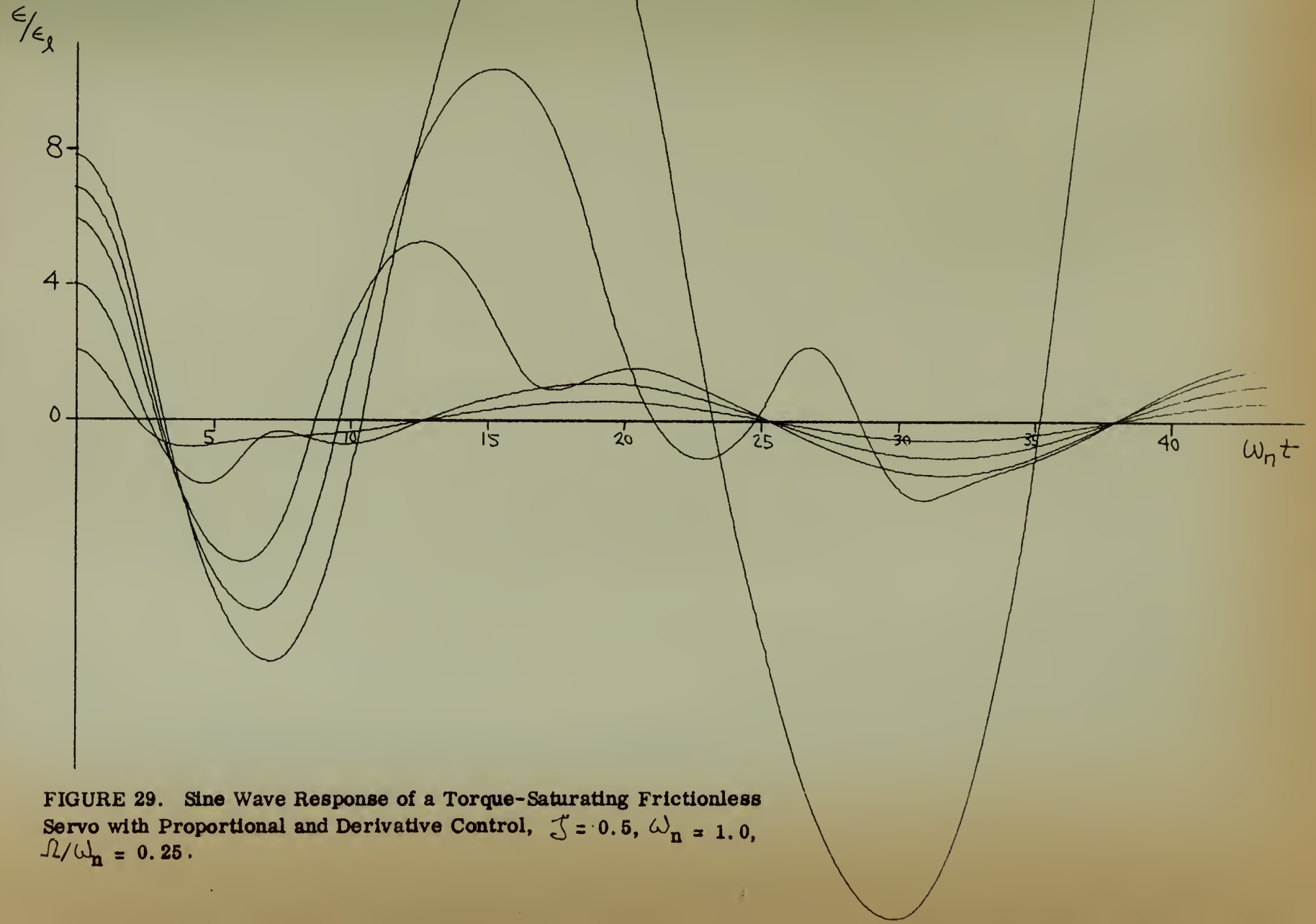

FIGURE 29. Sine Wave Response of a Torque-Saturating Frictionless Servo with Proportional and Derivative Control, $\zeta = 0.5$, $\omega_n = 1.0$, $\Omega/\omega_n = 0.25$.

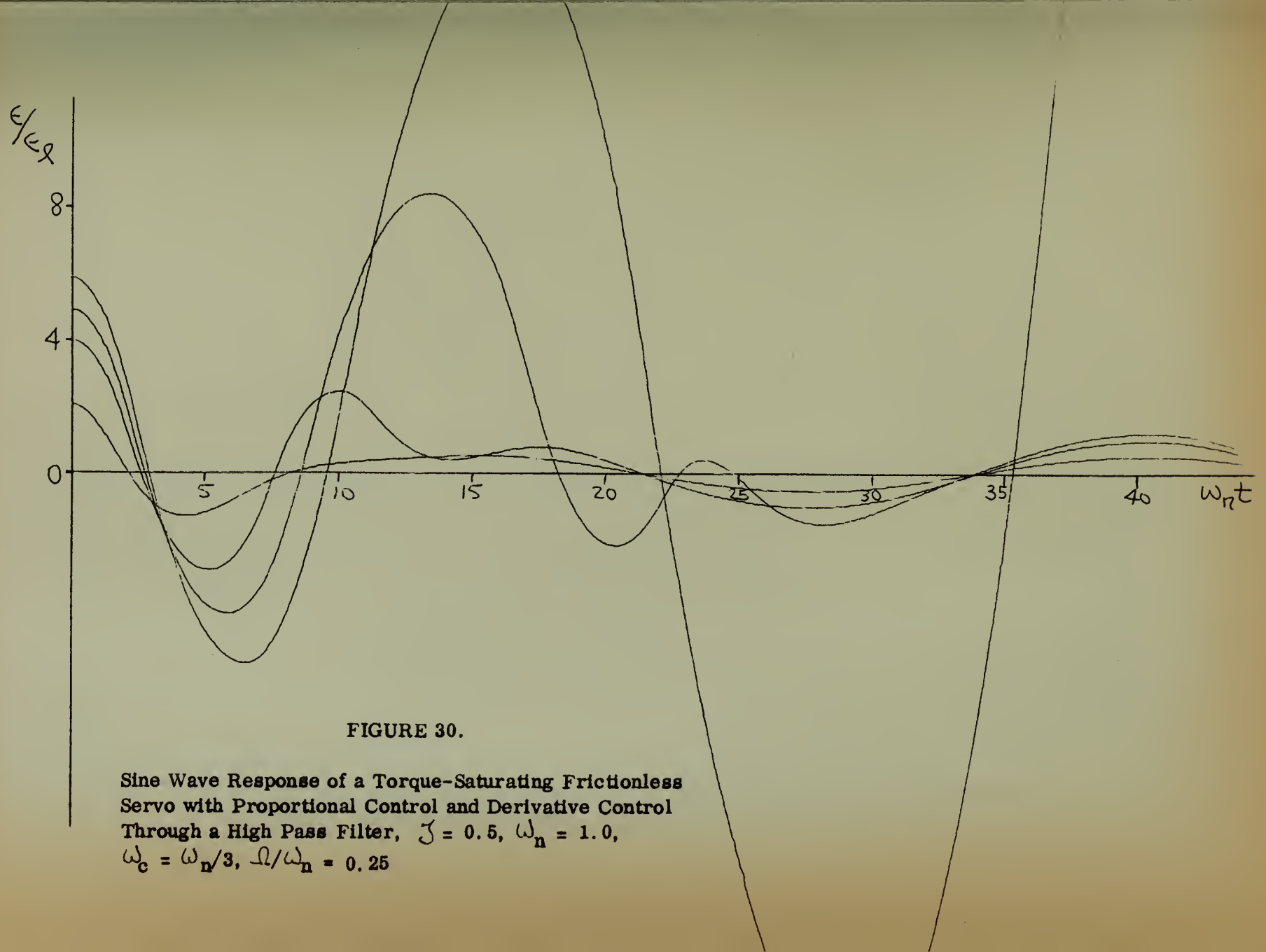

FIGURE 30.

Sine Wave Response of a Torque-Saturating Frictionless Servo with Proportional Control and Derivative Control Through a High Pass Filter, $\zeta = 0.5$, $\omega_n = 1.0$, $\omega_c = \omega_n/3$, $\Omega/\omega_n = 0.25$

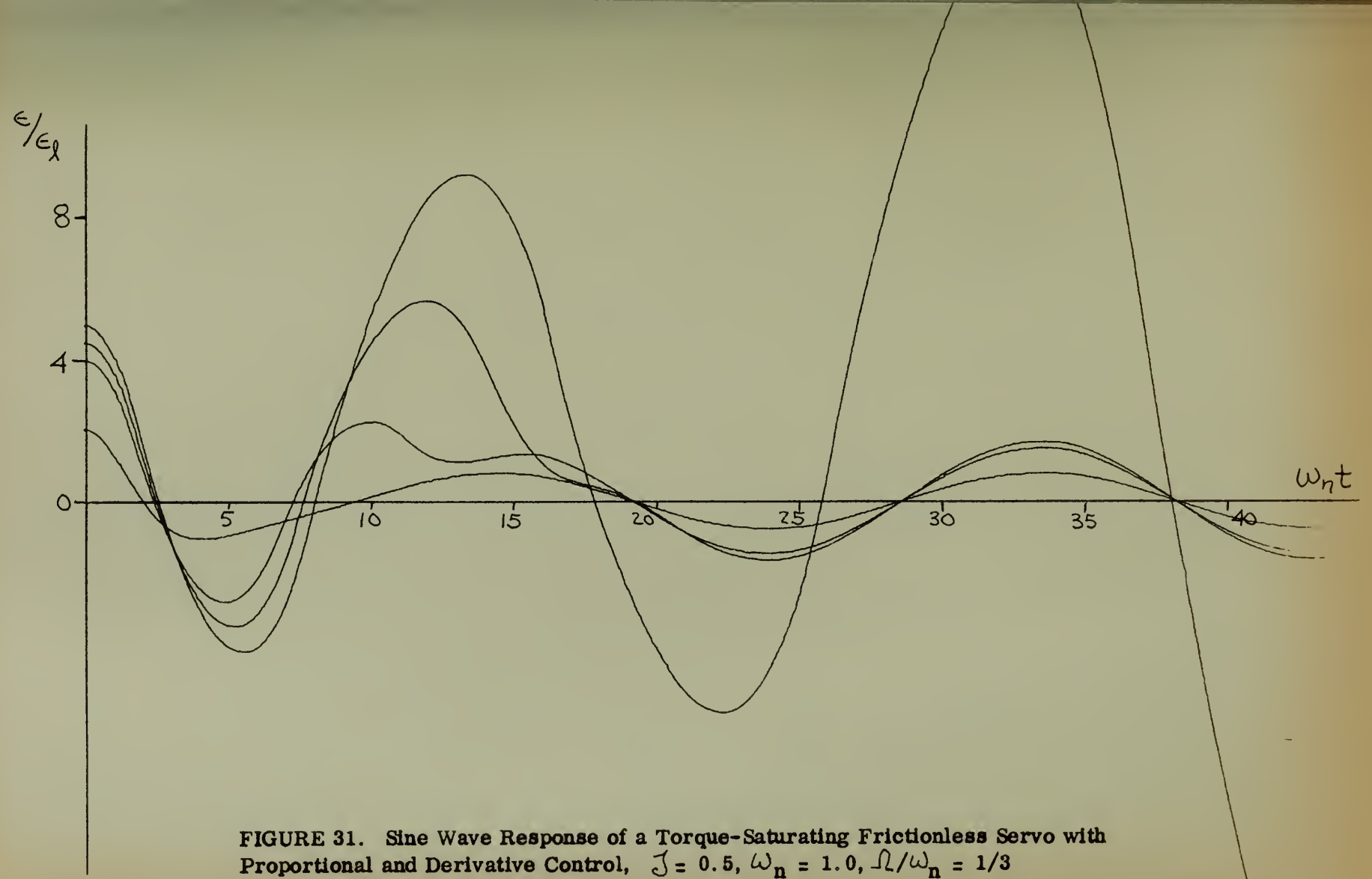

FIGURE 31. Sine Wave Response of a Torque-Saturating Frictionless Servo with Proportional and Derivative Control, $\mathcal{J} = 0.5$, $\omega_n = 1.0$, $\Omega/\omega_n = 1/3$

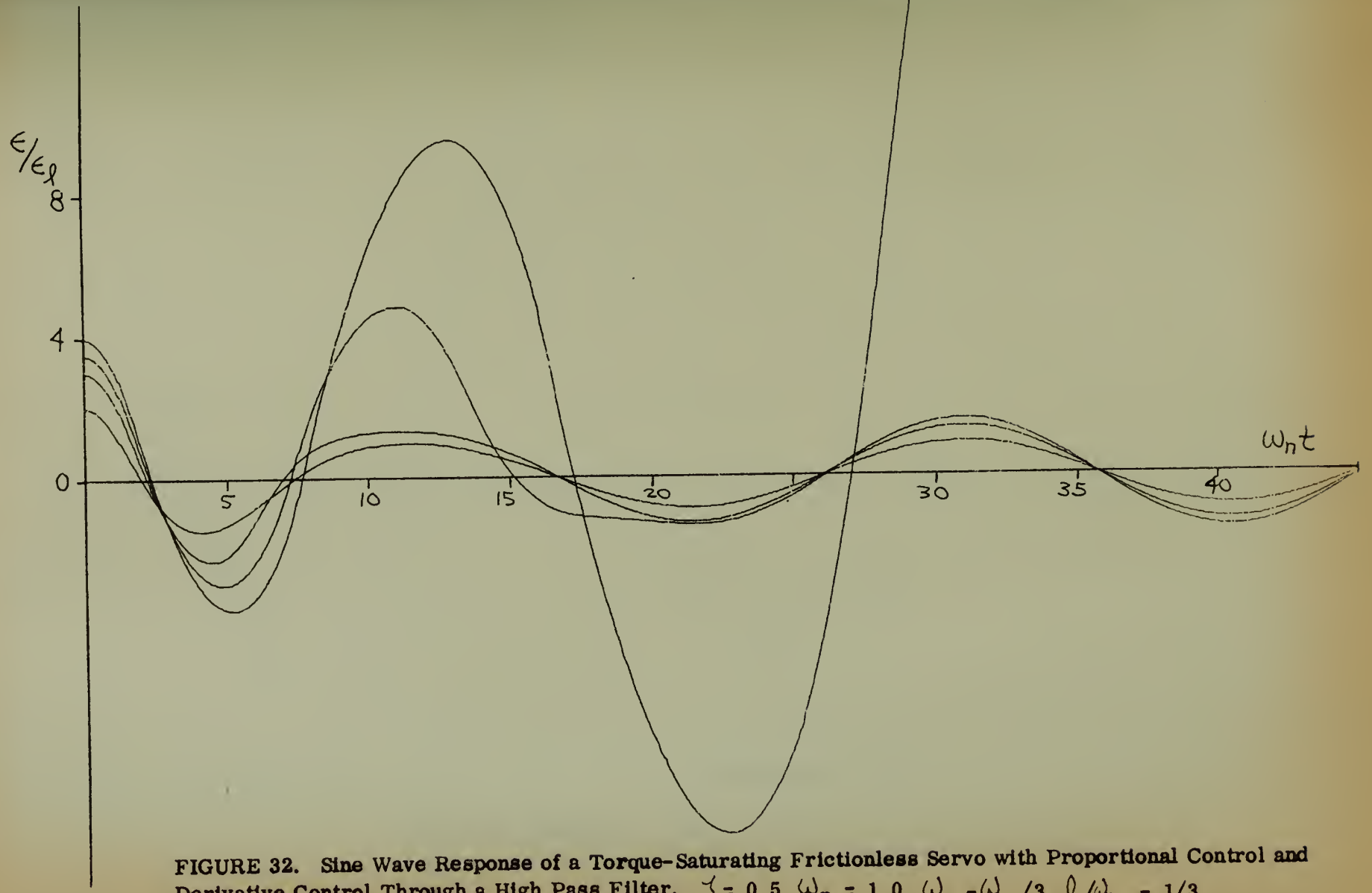

FIGURE 32. Sine Wave Response of a Torque-Saturating Frictionless Servo with Proportional Control and Derivative Control Through a High Pass Filter, $\mathcal{J} = 0.5$, $\omega_n = 1.0$, $\omega_c = \omega_n / 3$, $\Omega / \omega_n = 1/3$

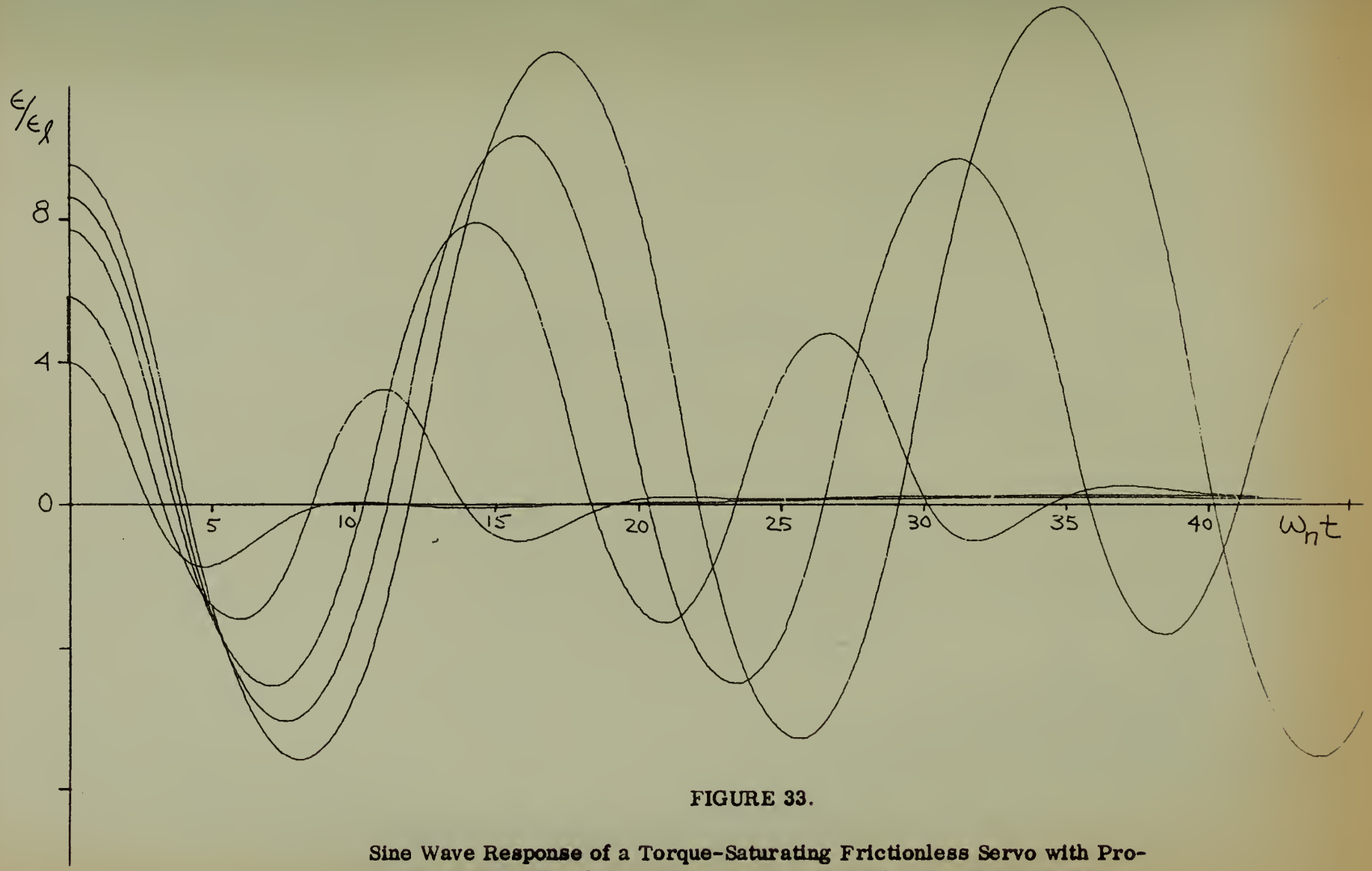

FIGURE 33.

Sine Wave Response of a Torque-Saturating Frictionless Servo with Proportional Control and Derivative Control Through a High Pass Filter, $\zeta = 0.5$, $\omega_n = 1.0$, $\omega_c = \omega_n/3$, $\Omega/\omega_n = 0.10$

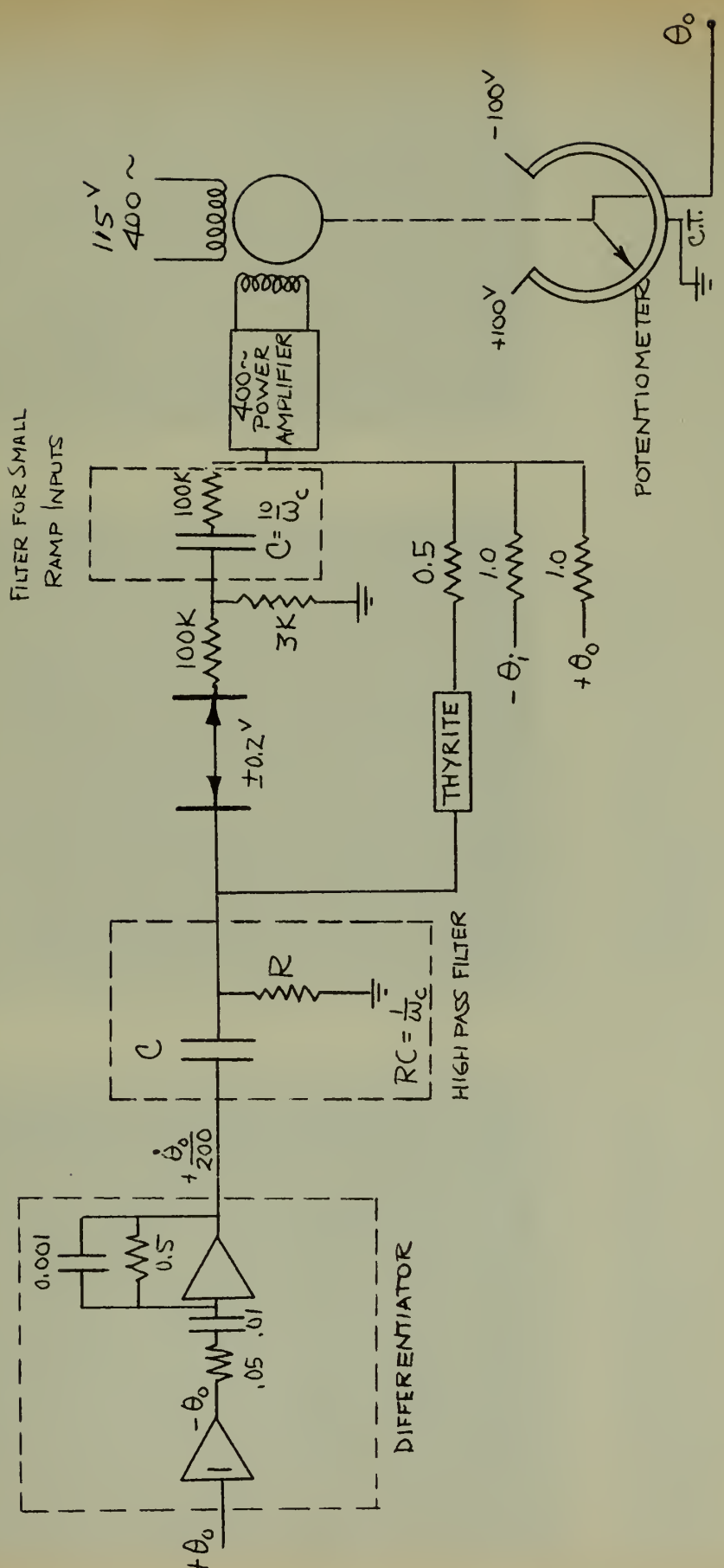

FIGURE 34. Servo Circuit Diagram.

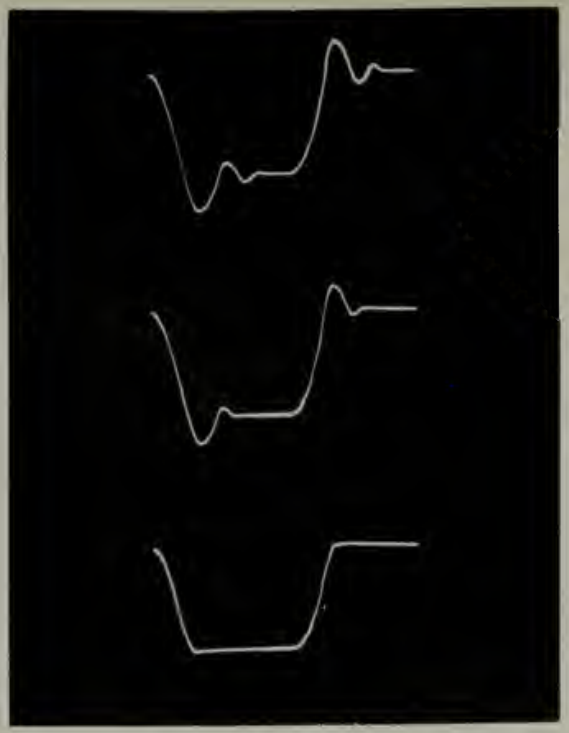

(a) 100^{V} Step: Proportional Control; Proportional plus Error-Rate Control; and Prediction, TOP to BOTTOM.

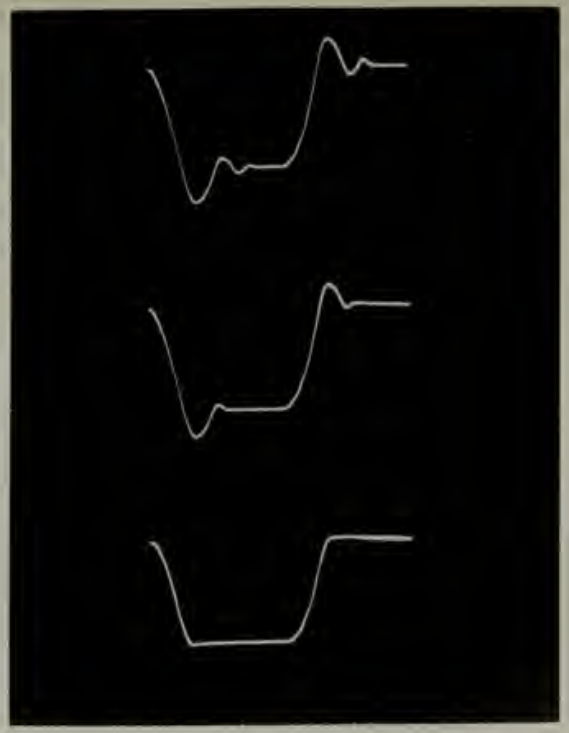

(b) 100^{V} Step: Proportional Control; Proportional plus Derivative Control; and Prediction, TOP to BOTTOM.

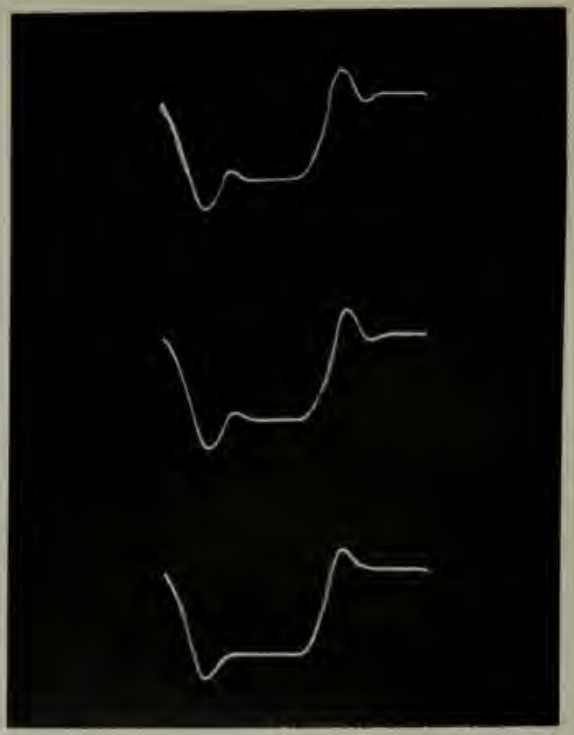

(c) 100^{V} Step: Proportional Control, Derivative Control and Prediction Through a High Pass Filter. $\omega_c = \omega_n/3$, $\omega_c = \omega_n/5$, $\omega_c = \omega_n/10$, TOP to BOTTOM.

FIGURE 35.

Step Responses of the Servo to Various Inputs.

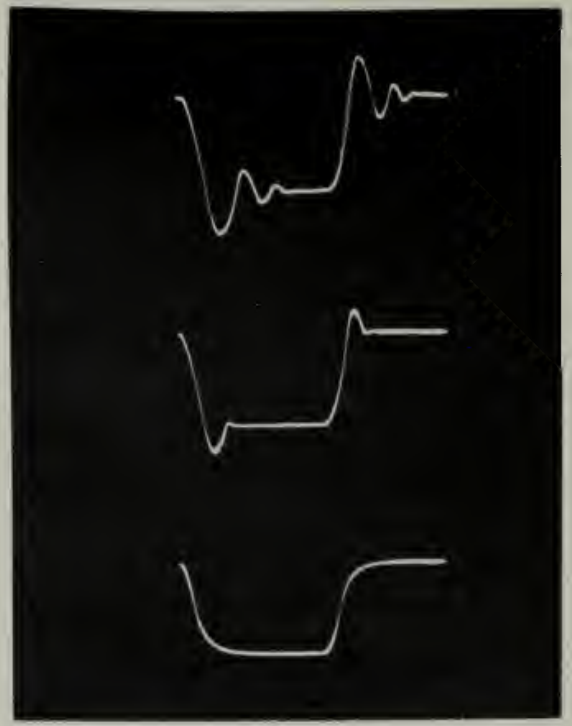

(a) 10^{V} Step: Proportional Control; Proportional plus Error-Rate Control; and Prediction, TOP to BOTTOM.

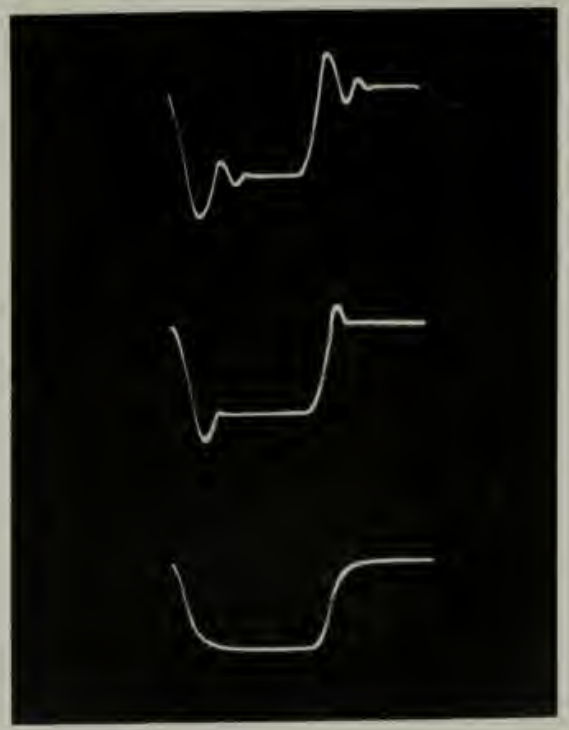

(b) 10^{V} Step: Proportional Control; Proportional plus Derivative Control; and Prediction, TOP to BOTTOM.

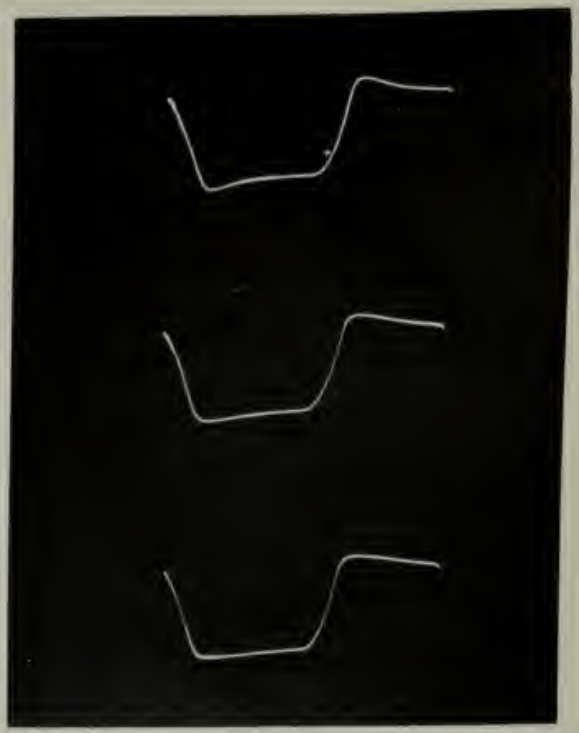

(c) 100^{V} Step: Proportional Control, Derivative Control and Prediction Through a High Pass Filter. $\omega_c = \omega_n/20, \omega_c = \omega_n/30, \omega_c = \omega_n/40$, TOP to BOTTOM.

FIGURE 36.

Step Responses of the Servo to Various Inputs.

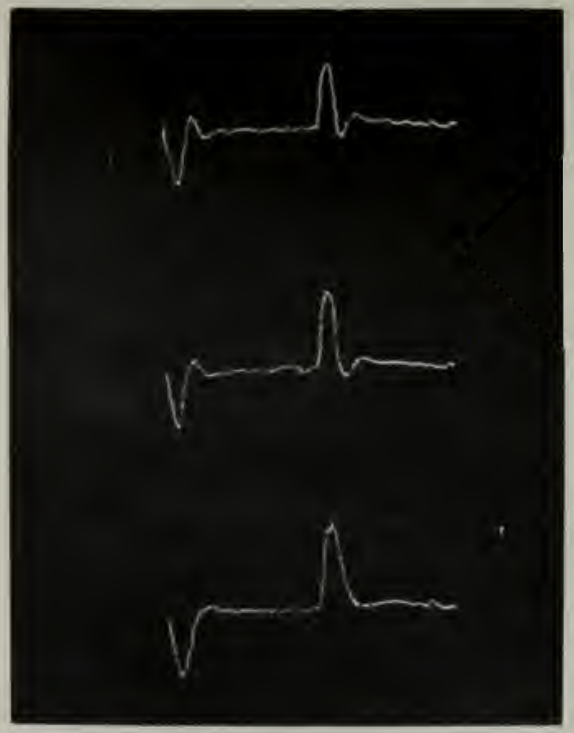

(a) Proportional Control, Derivative Control and Prediction Through a High Pass Filter. $\dot{\Theta}_i = 440^v/sec.$ $\omega_c = \omega_n/3$, $\omega_c = \omega_n/5$, $\omega_c = \omega_n/10$ TOP to BOTTOM.

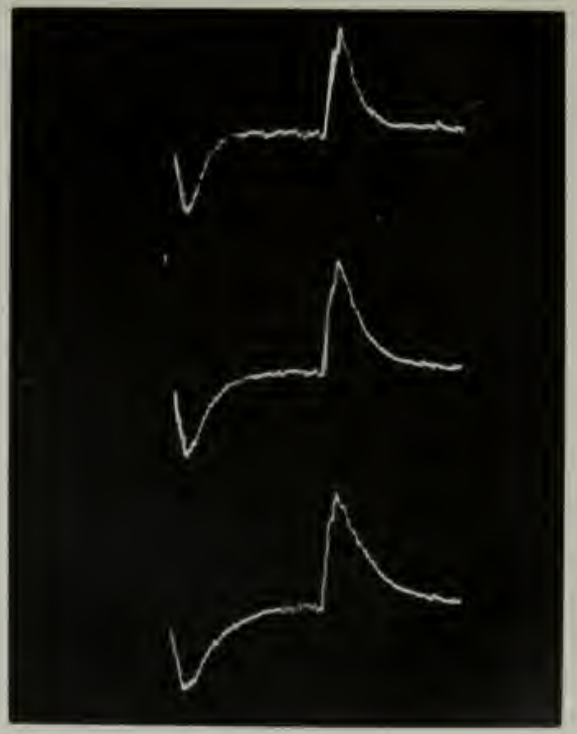

(b) Proportional Control, Derivative Control and Prediction Through a High Pass Filter. $\dot{\Theta}_i = 440^v/sec.$ $\omega_c = \omega_n/10$, $\omega_c = \omega_n/20$, $\omega_c = \omega_n/40$. TOP to BOTTOM.

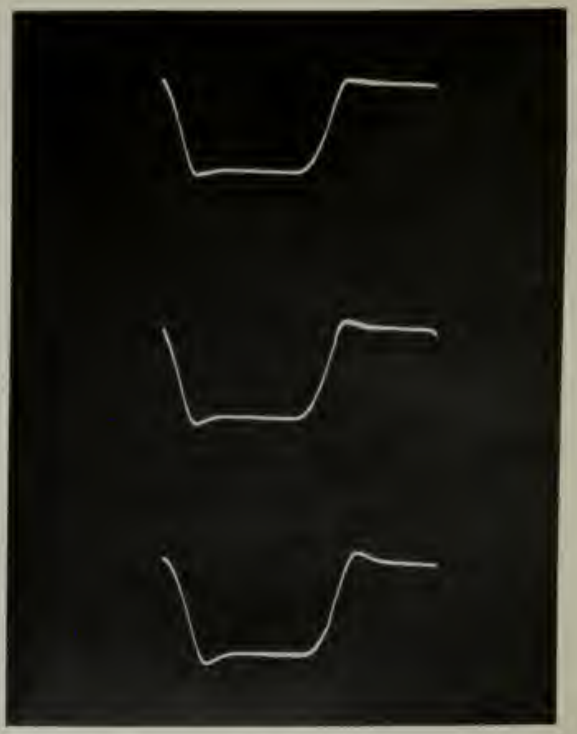

(c) 100^v Step Input: Proportional, Derivative Control Through a High Pass Filter and Prediction. $\omega_c = \omega_n/3$, $\omega_c = \omega_n/6$, $\omega_c = \omega_n/12$, TOP to BOTTOM.

FIGURE 37.

Responses of the Servo to Various Inputs.

REFERENCES

Ref. (A): McDonald, D. C., Nonlinear Techniques for Improving Servo Performance, Proc. Natl. Electronics Conf., Vol. 6, 1950, pp. 400-421.

Ref. (B): McDonald, D. C., Multiple Mode Operation of Servomechanisms, Rev. Sci., Inst., Vol. 23, Jan. 1952, pp. 22-30.

Ref. (C): Matthews, K. C., and Boe, R. C., The Application of Nonlinear Techniques to Servos, Proc. Natl. Elect. Conf., Vol. 8, 1952.

Ref. (D): Hopkin, A. M., A Phase Plane Approach to the Compensation of Saturating Servomechanisms, A. I. E. E. Tech. Paper, 51-103, 1951.

Ref. (E): Gay, W. W., and McCord, W. S., Optimum Prediction for a Torque-Saturating Servo, University of Michigan M. S. Thesis, Dept. of Aero. Engrg., May, 1956.

Ref. (F): Rauch, L. L., and Howe, R. M., A Servo with Linear Operation in a Region About the Optimum Discontinuous Switching Curve, Symposium on Nonlinear Circuit Analysis, April 25-27, 1956.

Ref. (G): Thyrite, A Nonlinear Resistance Material in which I Varies as E^n, General Electric Company, Metallurgical Products Div., Bulletin TY 101-5M-456, 1956.

Ref. (H): Kovach, L. D., and Comley, W., An Analog Multiplier Using Thyrite, Trans. I. R. E., Vol. EC-3, No. 2, pp. 42-45, June, 1954.

Ref. (I): Howe, R. M., Principals of Automatic Controls, Course Notes, AE 248, Dept. of Aero. Engrg., University of Michigan, Fall Term, 1956.

Ref. (J): Instruction Book for Reeves Electronic Analogue Computer C-101 MOD 5, Reeves Instrument Corporation, New York, pp. 53-57.

Ref. (K): Terman, F. E., Electronic and Radio Engineering, 4th Ed., McGraw-Hill, New York, 1955.

APPENDIX I

OPTIMUM SWITCHING CRITERIA

The technique developed in Ref. (F), combines the best features of the dual mode and continuous nonlinear feedback concepts as applied to optimization of servo response to a step input. Optimization results when minimum response time is realized. This can be accomplished by applying maximum torque for system acceleration, then reversing this maximum torque for decceleration, such that both the error and error-rate reduce to zero simultaneously. With no torque applied, the system then remains at rest until the next command signal.

A second-order system with output inertia only has a switching curve providing the required torque reversal characteristic for optimum response to step inputs as:

$$\epsilon + \frac{I}{2T_m}\left|\dot{\epsilon}\right|\dot{\epsilon} = 0. \qquad (1)$$

To have good overall performance, a controller must provide linear operation near the origin as well as torque reversal. Actually, a narrow strip adjacent the switching curve, (1), would provide for unsaturated operation within its limits throughout the phase space, and would allow linearity near the origin. For

$$\epsilon > \frac{I}{2T_m}\left|\dot{\epsilon}\right|\dot{\epsilon}$$

outside of this strip, make $I\ddot{\theta}_o = +T_m$, and for

$$\epsilon < \frac{I}{2T_m}|\dot{\epsilon}|\dot{\epsilon}$$

make $I\ddot{\theta}_o = -T_m$. Inside of the strip, it is necessary that $I\ddot{\theta}_o$ be a linear function of the displacement from the zero torque curve. Thus

$$I\ddot{\theta}_o = T_m \text{ sat } \left\{ \frac{\mu}{T_m}\left[\epsilon + \frac{I}{2T_m}|\dot{\epsilon}|\dot{\epsilon}\right]\right\} \qquad (2)$$

Equation (2) provides proportional feedback, but the damping vanishes as the error rate approaches zero. This loss in damping can be remedied by altering the shape of the zero torque curve so that it has a finite slope at the origin. This may be done by adding a saturated term in $\dot{\epsilon}$ to the switching curve, (1).

The equation of motion of the servo then becomes

$$I\ddot{\theta}_o = T_m \text{ sat}\left\{ \frac{\mu}{T_m}\left[\epsilon + \frac{T_m}{\mu} \text{ sat}\left(\frac{\mu C_e}{T_m}\dot{\epsilon}\right) + \frac{I}{2T_m}|\dot{\epsilon}|\dot{\epsilon}\right]\right\} \qquad (3)$$

Where: sat (X) = -1 for $X < -1$

X for $-1 \leqslant X \leqslant 1$

1 for $1 < X$

Equation (3) can be re-written in terms of the undamped natural frequency, ω_n, and the damping ratio, ζ, of the servo in the linear region. Thus

$$I\ddot{\theta}_o = T_m \text{ sat}\left\{\frac{1}{\epsilon_\ell}\left[\epsilon + \epsilon_\ell \text{ sat}\left(\frac{2\zeta}{\omega_n \epsilon_\ell}\dot{\epsilon}\right) + \frac{|\dot{\epsilon}|\dot{\epsilon}}{2\epsilon_\ell \omega_n^2}\right]\right\} \qquad (4)$$

Fig. I-1 shows this switching curve. From this curve, it is evident that a narrow linear region will give better utilization of the maximum torque operation.

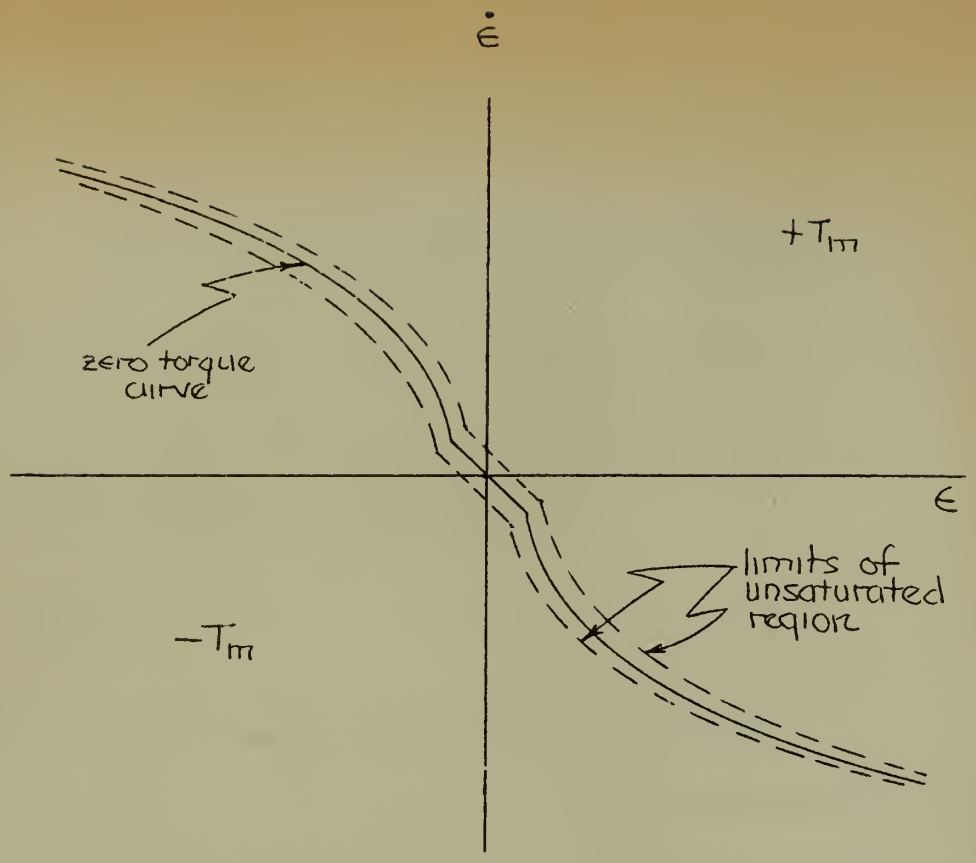

FIGURE I-1.

Phase Plane trajectory for the Optimum Switching Curve with Unsaturated Region.

APPENDIX II

THYRITE AS A NONLINEAR VOLTAGE ELEMENT

Thyrite is a nonlinear resistor in which the current varies as a power of the applied voltage. The expression which approximates the volt-ampere characteristic of a Thyrite resistor is

$$I = KE^n$$

where K = a constant (amperes at one volt), n = an exponent.

The exponent, n, varies from about 2.5 to 7, depending upon the manufacturing process.[G] (An ordinary linear resistor has an n of one.) To change the exponent to 2.0 for voltage squaring, it is necessary to place a linear resistor in series with the Thyrite. The volt-ampere characteristic becomes

$$E = IR_o + \left[\frac{1}{(K)^{1/n}} \right] I^{1/n}$$

Ref. (H) gives a method of calculating the best value of this series resistor, R_o. More rapid results can be obtained by merely inserting various values of series resistance until the desired exponent is approximately obtained.

Selection of a particular Thyrite resistor depends upon the resistance level and power ratings required for the application. Ref. (G) gives the volt-ampere characteristics of several Thyrite resistors. Typical characteristics for two representative resistors are reproduced in Fig. II-1.

Fig. II-1 indicates that G. E. Cat. No. 8396839 G1 has an n most

nearly that of the desired exponent, n = 2, although its input voltage rating is quite low. For this reason, G. E. Cat. No. 8386118 G2 was investigated for the squaring application. It was observed that a reduction in applied

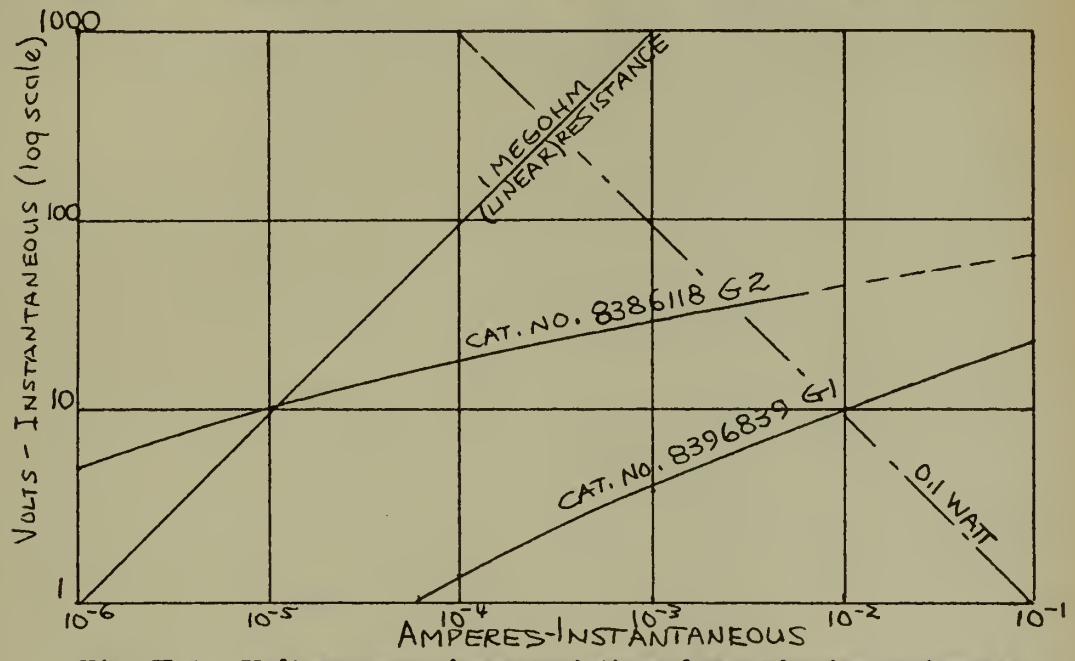

Fig. II-1. Volt-ampere characteristics of two Thyrite resistors.

voltage resulted in a reduction in exponent. An input of less than about five volts result in an exponent of approximately 2 for the higher rated resistor. Table II-1 shows this Thyrite resistor with a 15 megohm linear resistor in series. Figure II-2 is a representative plot of these characteristics and shows the anti-symmetrical nature of the Thyrite, resulting in an output, the sign of which is dependent upon the sign of the input voltage. This particular characteristic is ideal for the bi-directional characteristic of a square law predictor.

Table II-1 indicates an accuracy in voltage squaring of 0.50% of full scale up to an input voltage of 20 volts, for G. E. Cat. No. 8386118 G2. Ref. (H) indicates that G. E. Cat. No. 8396839 G1 is capable of an accuracy of

0.125% of full scale when operated up to a maximum of about 15 volts.

Input volts	Output volts	Desired output volts	Full scale (100^{V}) Percentage Error
1	0.010	0.010	0
2	0.039	0.040	-0.001
4	0.162	0.160	+0.002
6	0.372	0.360	0.012
8	0.664	0.640	0.024
10	1.060	1.000	0.060
12	1.570	1.440	0.130
14	1.970	1.960	+0.010
16	2.480	2.560	-0.080
18	3.070	3.240	-0.170
20	3.500	4.000	-0.500
30	6.330	9.000	-2.670

Table II-1. Voltage Characteristic of G. E. Cat. No. 8386118 G2 Thyrite with insertion loss of 100.

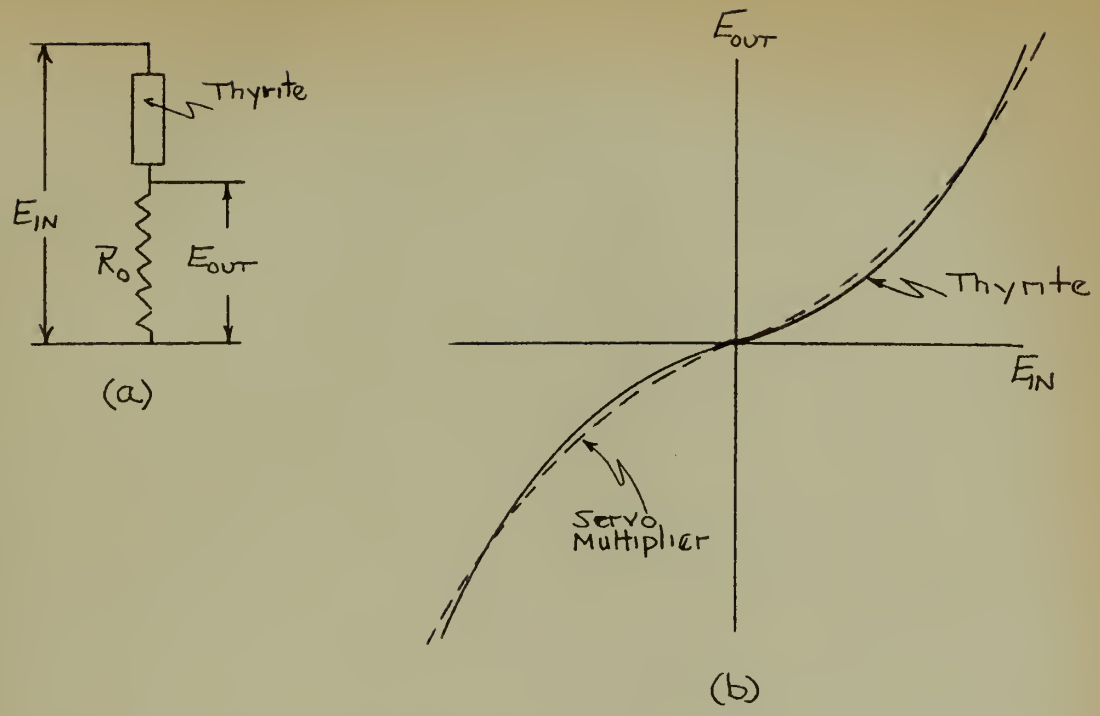

Fig. II-2. Anti-symmetrical Squaring Characteristic for G. E. Cat. No. 8386118 G2 Thyrite.

35900

Thesis
M62
c.1

Minnis
A passive element non-
linear controller for
torque-saturating servos.